535
8-21-78

Ch. 403

COO-2607-5

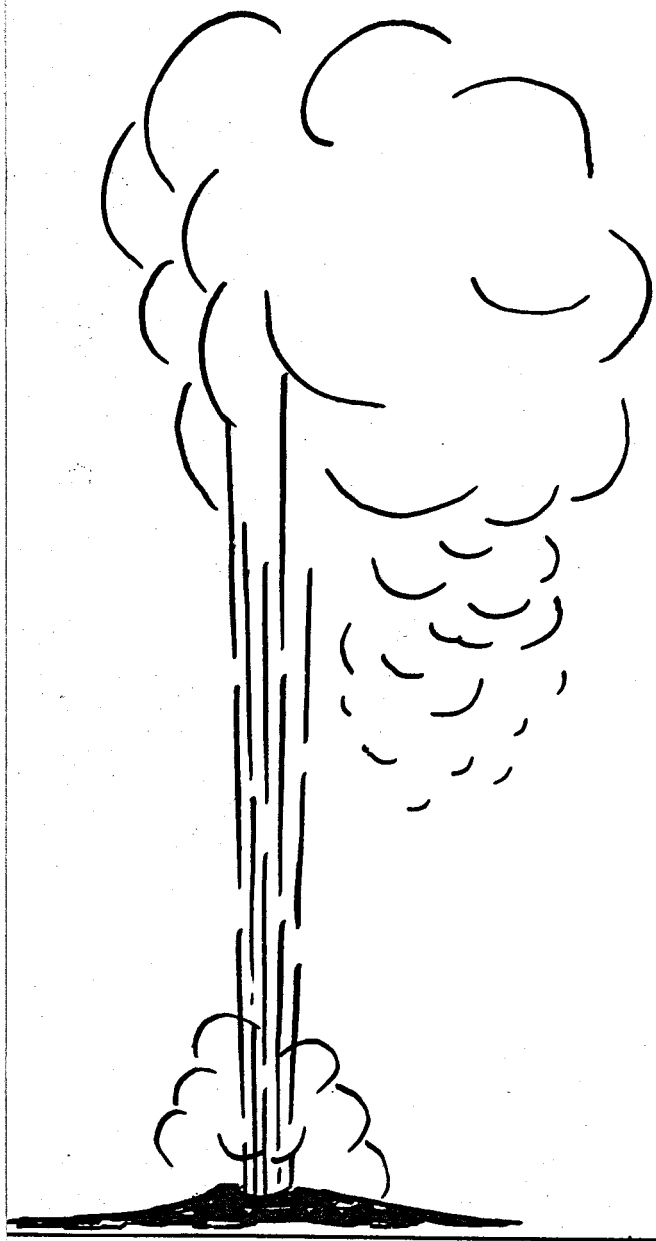

STUDY OF SILICA SCALING FROM GEOTHERMAL BRINES

Final Report, November 15, 1974—April 30, 1977

By
A. C. Makrides
M. J. Turner
W. W. Harvey
J. Slaughter
S. B. Brummer
P. O'D. Offenhartz
G. F. Pearson

January 1978

Work Performed Under Contract No. EY-76-C-02-2607

EIC Corporation
Newton, Massachusetts

U. S. DEPARTMENT OF ENERGY
Geothermal Energy

DISCLAIMER

NOTICE

COO-2607-5
Distribution Category UC-66d

STUDY OF SILICA SCALING FROM GEOTHERMAL BRINES

Final Report
for Period November 15, 1974 - April 30, 1977

A. C. Makrides
M. J. Turner
W. W. Harvey
J. Slaughter
S. B. Brummer
P. O'D. Offenhartz
G. F. Pearson

EIC Corporation
55 Chapel Street
Newton, Massachusetts 02158

January 1978

Prepared for

U.S. DEPARTMENT OF ENERGY
UNDER CONTRACT NO. EY-76-C-02-2607

ABSTRACT

Condensation of silica from brines supersaturated in silicic acid was studied over a range of pH (4.5-6.5), temperature (75°-105°C), salinity, and silicic acid concentration (700 to 1200 ppm as SiO_2). The experimental technique involved analyses for molybdate-reactive silicic acid as a function of time after a supersaturated solution of $Si(OH)_4$ was prepared by mixing aliquots of a stock silicate solution with buffered brine.

The isothermal rate of SiO_2 condensation is a strong function of supersaturation (C/C_e), pH, and salinity. The overall kinetics follow what is expected from the general theory of phase transitions. At supersaturations less than about 3, there is an apparent transition period during which the rate of removal of silicic acid from solution is below the detection limit of the analytical technique. This period amounts to several hundred minutes at supersaturations of about 2.0.

The kinetic results suggest that growth of nucleated particles is activation controlled, at least initially. The primary nuclei have radii of the order of a few angstroms. Particles of several hundred angstroms are produced eventually.

The increase of condensation rate with salt content is attributed to a decrease in equilibrium solubility of SiO_2. In effect, higher salt concentrations increase supersaturation and lead to faster nucleation.

Higher nucleation and growth rates are observed at higher pH's. An increase of 1 pH unit increases rates by a factor of about 10. The pH dependence is consistent with the hypothesis that $SiO(OH)_3^-$ is one of the reacting species.

Temperature (75°-105°C) has little effect on condensation rate at a fixed initial silicic acid concentration. This result suggests that the increase in rate of activated steps brought about by increased temperature is essentially counterbalanced by a decrease in supersaturation (because of higher equilibrium solubility at higher temperatures).

The kinetic results yield an activation energy of 17 kcal/mol for addition of silicic acid to a nucleated particle and 45 ergs/cm^2 for the interfacial energy between precipitated silica and the brine.

NaCl, KCl, $CaCl_2$ and $MgCl_2$ had no specific effect on condensation rate. However, NaF had a large effect on rate; a few ppm (15-100) of fluoride ion accelerate condensation substantially.

TABLE OF CONTENTS

TABLE OF CONTENTS
(Continued)

LIST OF FIGURES

LIST OF FIGURES
(Continued)

I. INTRODUCTION

A study of mechanisms of condensation of silica from simulated geothermal brines was carried out to establish a basis for controlling scaling problems in geothermal power production.

A generalized scheme for formation of scale from silicic acid is shown in Figure 1. There are two major pathways for scale formation: heterogeneous nucleation (on the surface of interest) followed by growth, and homogeneous nucleation in solution with deposition of colloidal silica. The work described here is concerned with homogeneous condensation and growth.

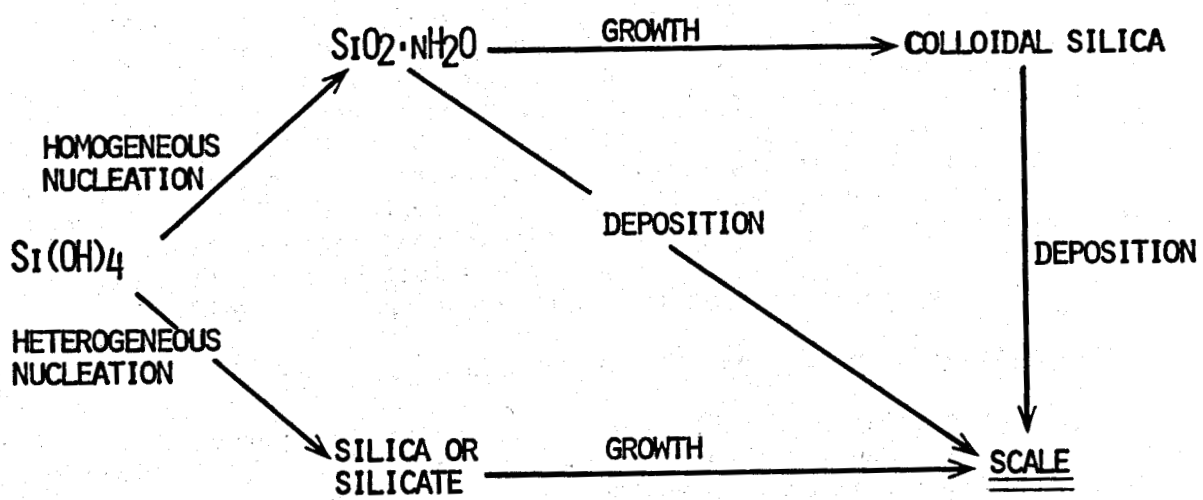

Fig. 1: Homogeneous and heterogeneous pathways for scale formation.

The term "homogeneous nucleation" is somewhat misleading since the system is clearly heterogeneous as soon as the second phase, amorphous silica, appears. The use of the term conveys that nucleation occurs out of a homogeneous solution and does not involve a second phase, for example, a particle of dust. As with other condensation phenomena, we expect that important variables include supersaturation and temperature. In the particular case of silica condensation, the pH is another variable with major influence on kinetics. As will become evident subsequently, salt concentration also plays a significant role in condensation kinetics, primarily because of its effect on equilibrium solubility of amorphous silica. Finally, at least one other ion, namely fluoride, has a specific and significant effect on condensation kinetics.

II. EXPERIMENTAL

1. Introduction

In the systems of interest, namely geothermal brines, silica is in monomeric form having originated from dissolution of quartz (1). These solutions become supersaturated principally as a consequence of temperature decrease associated with thermal energy extraction. Supersaturation is further increased by flashing, which concentrates the brine in the non-volatile components.

Preparation in the laboratory of supersaturated solutions of silica monomer presents some difficulties. Supersaturated solutions can be obtained by quenching high temperature brines equilibrated with quartz. This procedure, although used elsewhere (see, for example, ref. 2), is cumbersome and imposes a limit on the silica concentration that can be achieved. It also presents difficulties in precise control of solution pH and salt composition. An alternative approach, used in this work, is to prepare a supersaturated solution at the desired temperature by mixing an alkaline solution of sodium silicate with a buffered brine so as to obtain a final solution of the desired silicic acid concentration, pH, and salinity. In this case, mixing conditions must be controlled carefully to avoid artifacts arising from the mixing process itself.

2. Preparation of Supersaturated Silica Solutions

Simulated brines supersaturated in silica were prepared by acidification of aliquots of the stock sodium silicate solution. The stock silica solution (containing about 1700 to 2000 ppm SiO_2) and the acidified brines were thermostated in an oil bath at temperatures in the range 75° to 105°C. After thermal equilibration, the stock solution was added to the brine as a thin stream under vigorous stirring. Transfer was accomplished by pressurizing the stock solution with N_2. The total transfer time was 10-30 sec; the temperature fluctuation during transfer was less than 2°C.

The acidified brine contained NaCl, KCl, and varying amounts of HCl, NaAc, and HAc (where Ac = acetate). Since the silicate solution is alkaline (pH $\sim$13), the composition of the brine must be adjusted to obtain at each silica concentration the desired final pH (in the range 4.5 to 6.5) and total salt concentration. The adjustment was made by a preliminary titration (at room temperature) of a brine containing the desired amount of silicate. With the help of such adjustments, we were able to control the final pH of the supersaturated silicic acid solution to within ± 0.05 pH unit.

A detailed discussion of the preparation of supersaturated solutions is given in Appendix A.

3. Analytical Procedures

The determination of silicic acid concentration was based on the β-complex of silicic acid with molybdate (3) and generally followed the method recommended by Alexander (4). The major modification was in the acidification step. In the procedure described by Alexander (4), acidification is carried out at 2°C and the total concentration is limited to less than 1.0 mg/ml of SiO_2. As has been observed by others (5) and confirmed by us, this procedure leads to a nonlinearity of absorbance as a function of $Si(OH)_4$ concentration. A change to an acidification procedure which limits the total concentration to less than 0.15 mg/ml resolves this difficulty. Acidification within this concentration limit is preferably carried out at room temperature (∿25°C) rather than at 2°C. The overall analytical procedure is described in Appendix B.

4. Other Experimental Conditions

Two buffers were used - acetic acid/acetate for pH in the range 4.5 to 5.5 and maleic acid/maleate in the range 5.5 to 6.5. Kinetic runs for silica condensation at pH = 5.50 using acetate and maleate buffers yielded essentially identical results.

The pH values given in the text were measured at room temperature (∿25°C). Over the temperature range investigated (25° to 105°C), pH varies by less than 0.1 unit (see Appendix A).

Reaction vessels and auxiliaries were of Teflon. Other containers were of polyethylene. Glass did not come into contact with any of the supersaturated silica solutions. Silica stock solutions were made up to volume in Pyrex volumetric flasks and stored in polyethylene containers.

Observed absorbances in the spectrophotometric determination of dissolved silica in aliquots taken during condensation runs were corrected for light scattering by suspended SiO_2 particles. Corrections for light scattering were negligible in the initial stages of condensation but amounted to as much as 10% in the final stages of condensation. It should be noted that since 100 µl of sample was injected in 3.0 cc of molybdate reactant, the light scattering correction was 1/30 of the scattering observed for the acidified, undiluted sample.

III. RESULTS

1. Introduction

Brines supersaturated in silica were prepared as described in the experimental section, and the rate of condensation of silicic acid was followed by removing aliquots periodically and analyzing for molybdate-reactive silicic acid. The concentration of molybdate-reactive silicic acid at pH = 4.50 and 95°C is shown as a function of time in Figure 2.

Molybdate-reactive silica includes monosilicic and disilicic acids. Higher condensed species do not contribute significantly to the total amount of silica in solution as determined by the analytical technique we used. In fact, we may assume with negligible error that the concentration of silica determined by reaction with molybdate is the sum of monomeric and dimeric silicic acid. We will refer to this sum as "dissolved silica" and represent it by $[Si(OH)_4]$.

Several features of Figure 2 are noteworthy. The rate of condensation is a strong function of initial concentration of $Si(OH)_4$. At initial concentrations of about 1100 ppm (as SiO_2) or less, a transition period is evident during which there is little loss of dissolved silicic acid from solution. Subsequently, the condensation rate becomes appreciable and the main part of the reaction is essentially over in a relatively short time. The duration of the apparent transition period decreases as the initial silicic acid concentration increases.

Approach to equilibrium solubility is relatively slow. Typically, 24 hours or more are required at 95°C. Equilibrium solubilities are achieved faster from solutions having greater initial silicic acid concentrations. These features of the condensation process are evident at all pH's, temperatures, and salinities, as will become apparent from results presented below.

The general features described above, particularly the strong dependence on initial concentration, are characteristic of condensation (precipitation) reactions and suggest that the results can be treated by classical condensation theory. The first question that arises is whether nucleation occurs essentially during the mixing process or whether it takes place throughout the initial phases of the reaction. The series of experiments undertaken to elucidate this point and the corresponding analytical tests are given in Appendix C. Based on these results, we concluded that nucleation during the mixing process makes only a small contribution to the total number of nuclei eventually formed. The main

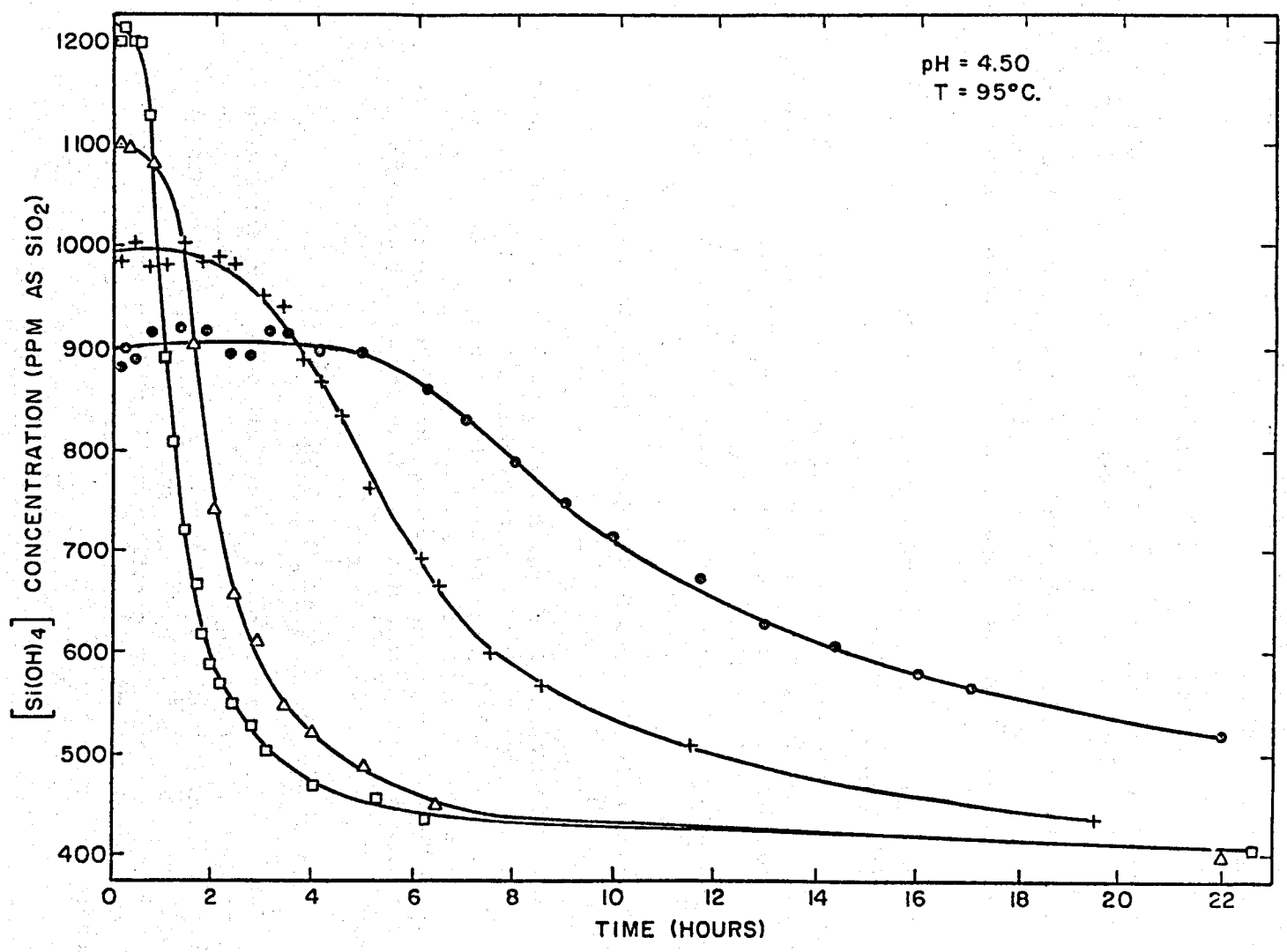

Fig. 2: Silica condensation as a function of time for a series of initial silicic acid concentrations.

part of the nucleation process occurs after mixing has taken place and continues as long as the supersaturation is sufficiently large to yield appreciable nucleation rates.

2. Condensation Kinetics at pH = 4.50 and 95°C

The general condensation curve was given in Figure 2. Results during the initial period are shown on an expanded time scale in Figure 3.

A brine with composition 0.065M KCl, 0.250M NaCl, 0.202M NaAc and 0.216M HAc (pH = 4.50) was routinely used and is referred to as the standard brine. At pH = 5.50 the composition of the standard brine was the same, except that HAc was 0.012M.

3. Condensation Kinetics at pH = 4.50, T = 95°C and Varying Salinities

Kinetics of condensation at a fixed initial concentration of silicic acid equal to 1100 ppm as SiO_2 and at varying salinities (chloride ion concentration 0.15 to 1.55M) are given in Figure 4. As is evident from the figure, the initial transition period decreases as salinity increases. The rate of the subsequent condensation process is greater at higher salinities.

4. Condensation Kinetics in Standard Brine at pH = 4.50 and Various Temperatures

Kinetics of condensation in the standard brine at a fixed, initial concentration of 1100 ppm as SiO_2 were determined at a series of temperatures from T = 75°C to 105°C. The results are given in Figure 5. In general, the effect of temperature is small. The initial transition period is only slightly dependent on temperature; the rate of the subsequent condensation process is not a strong function of temperature from 75° to 105°C.

5. Condensation Kinetics at pH = 5.50 and 95°C

Standard brines supersaturated in silicic acid were prepared as before except that the pH was adjusted to 5.50. The kinetics of condensation at this pH are shown in Figures 6 and 7. In general, results are analogous to those obtained at pH = 4.50 except that the rate, at any given initial silicic acid concentration, is significantly greater at pH 5.50 than at pH 4.50. The comments made above on results at pH 4.50 are applicable here also.

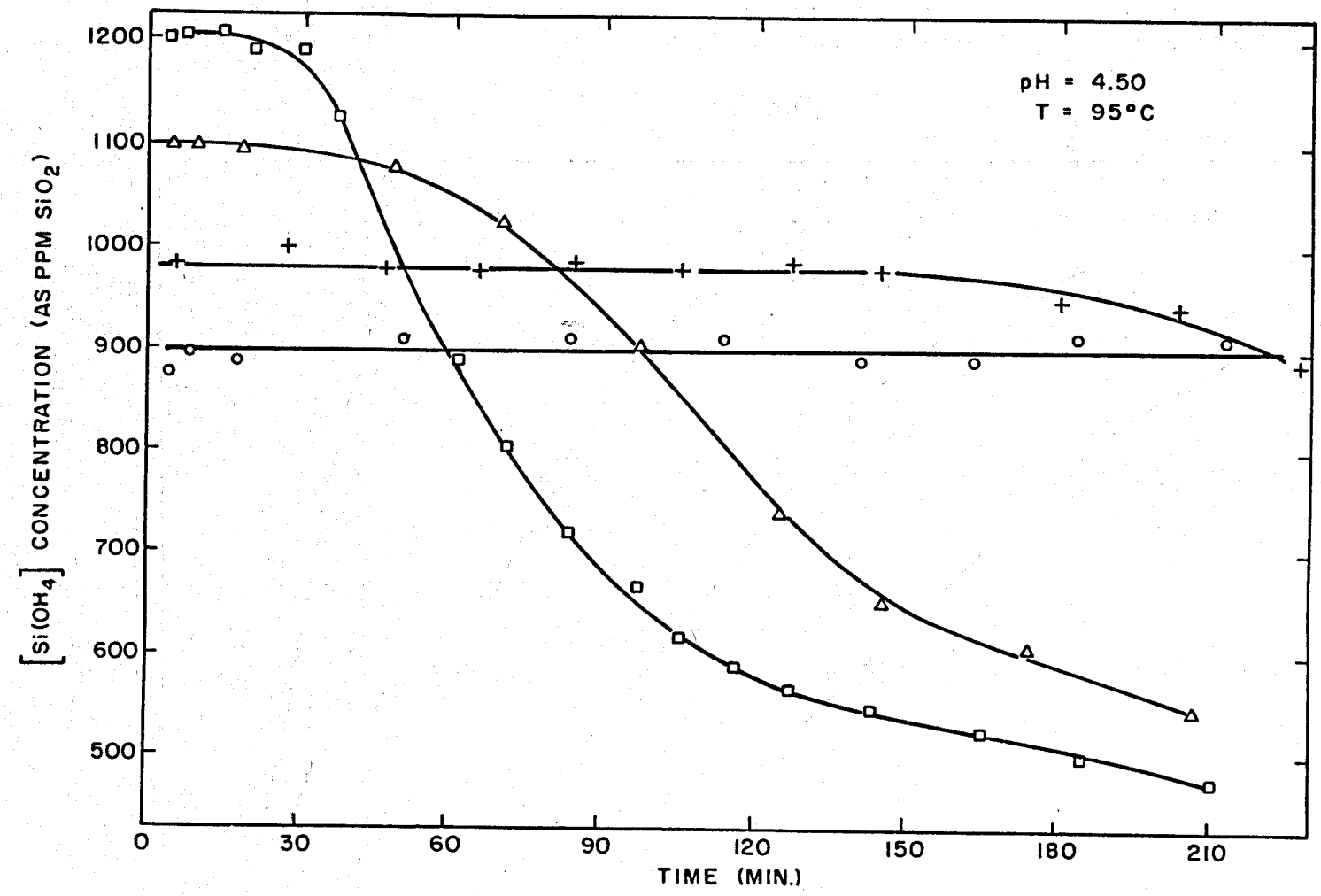

Fig. 3: Silica condensation as a function of time for a series of initial silicic acid concentrations.

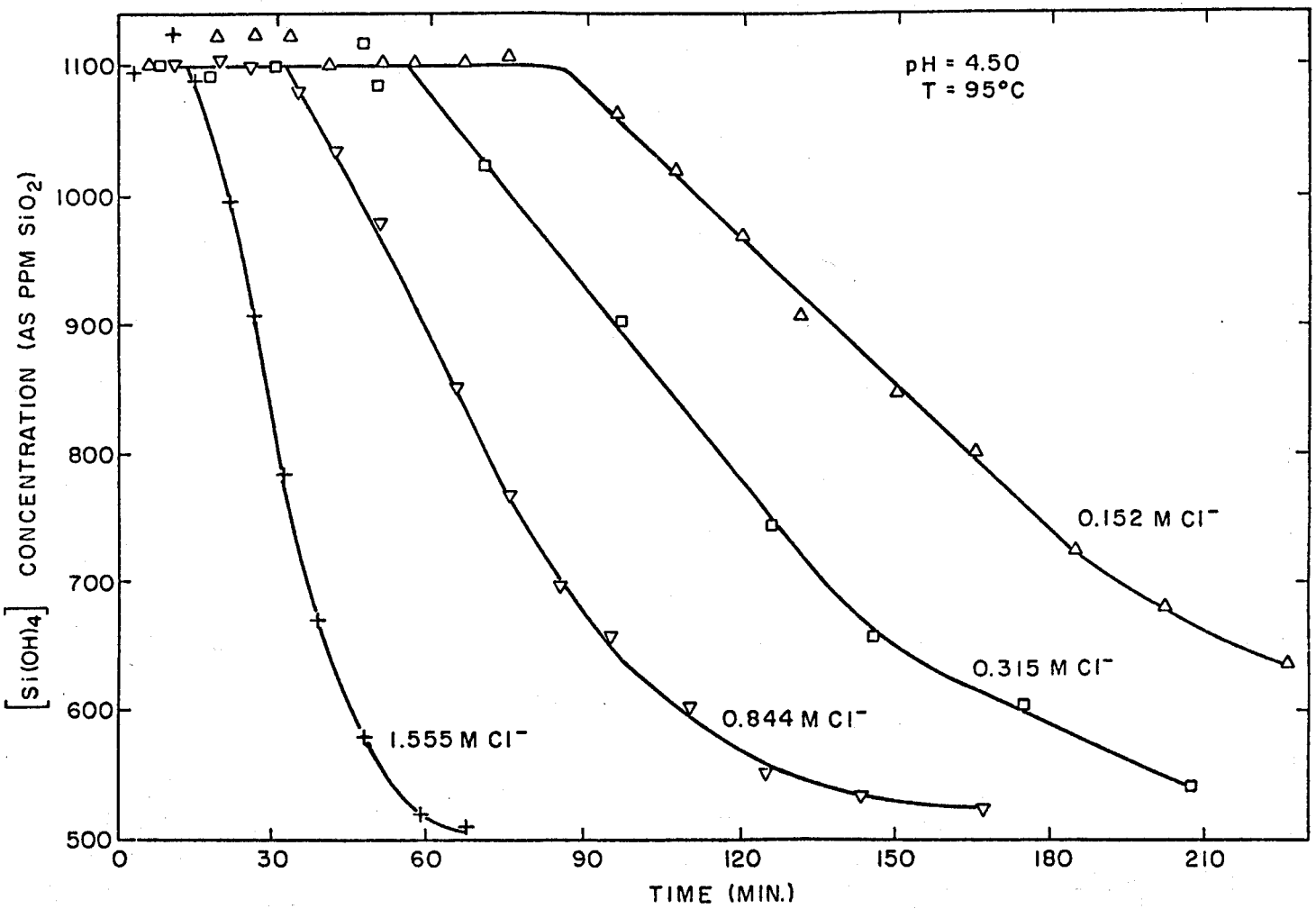

Fig. 4: Silica condensation from a solution of 1100 ppm (as SiO_2) initial concentration as a function of time at various salinities.

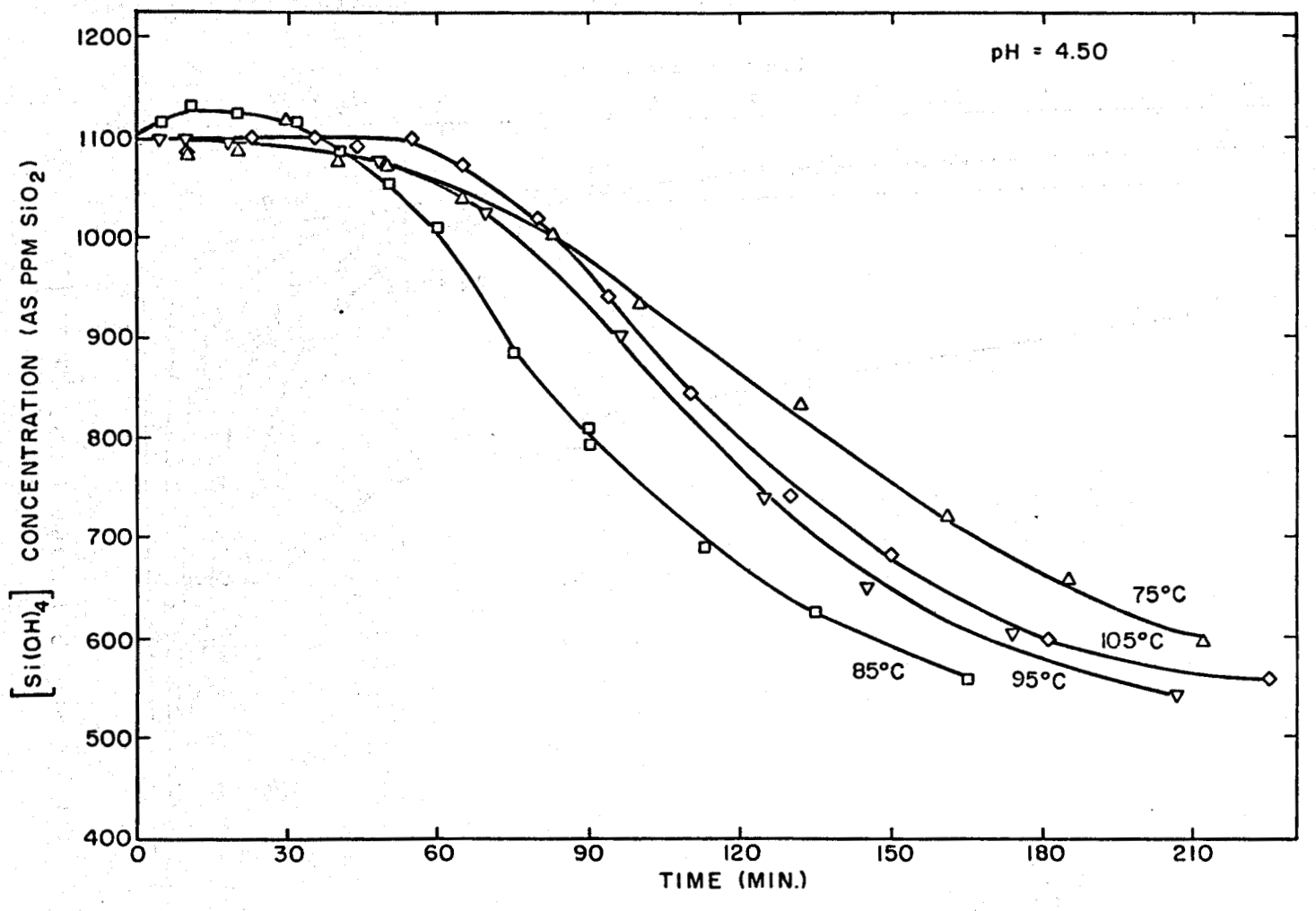

Fig. 5: Silica condensation from a solution of 1100 ppm (as SiO_2) initial concentration as a function of time at various temperatures.

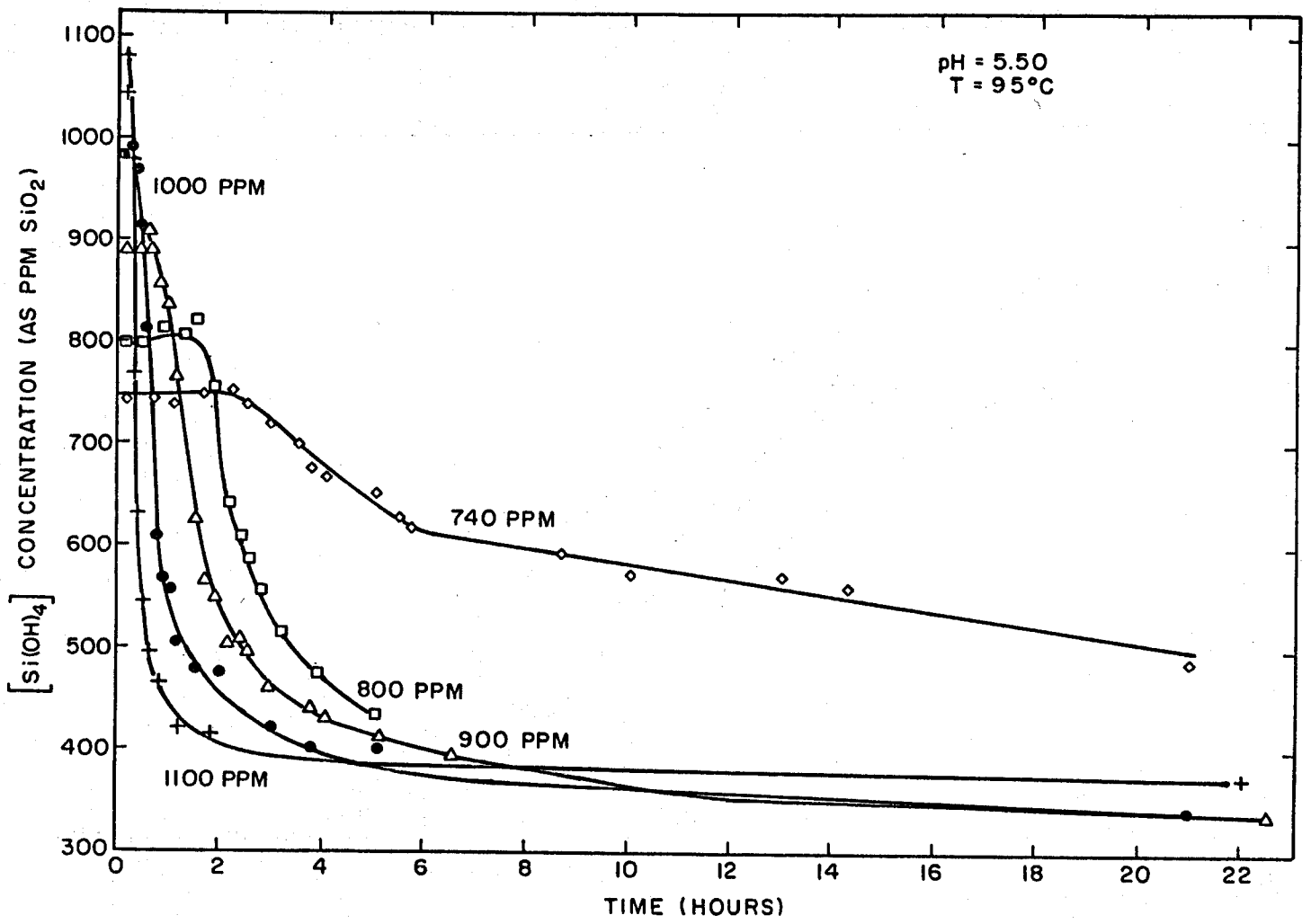

Fig. 6: Silica condensation as a function of time for a series of initial silicic acid concentrations.

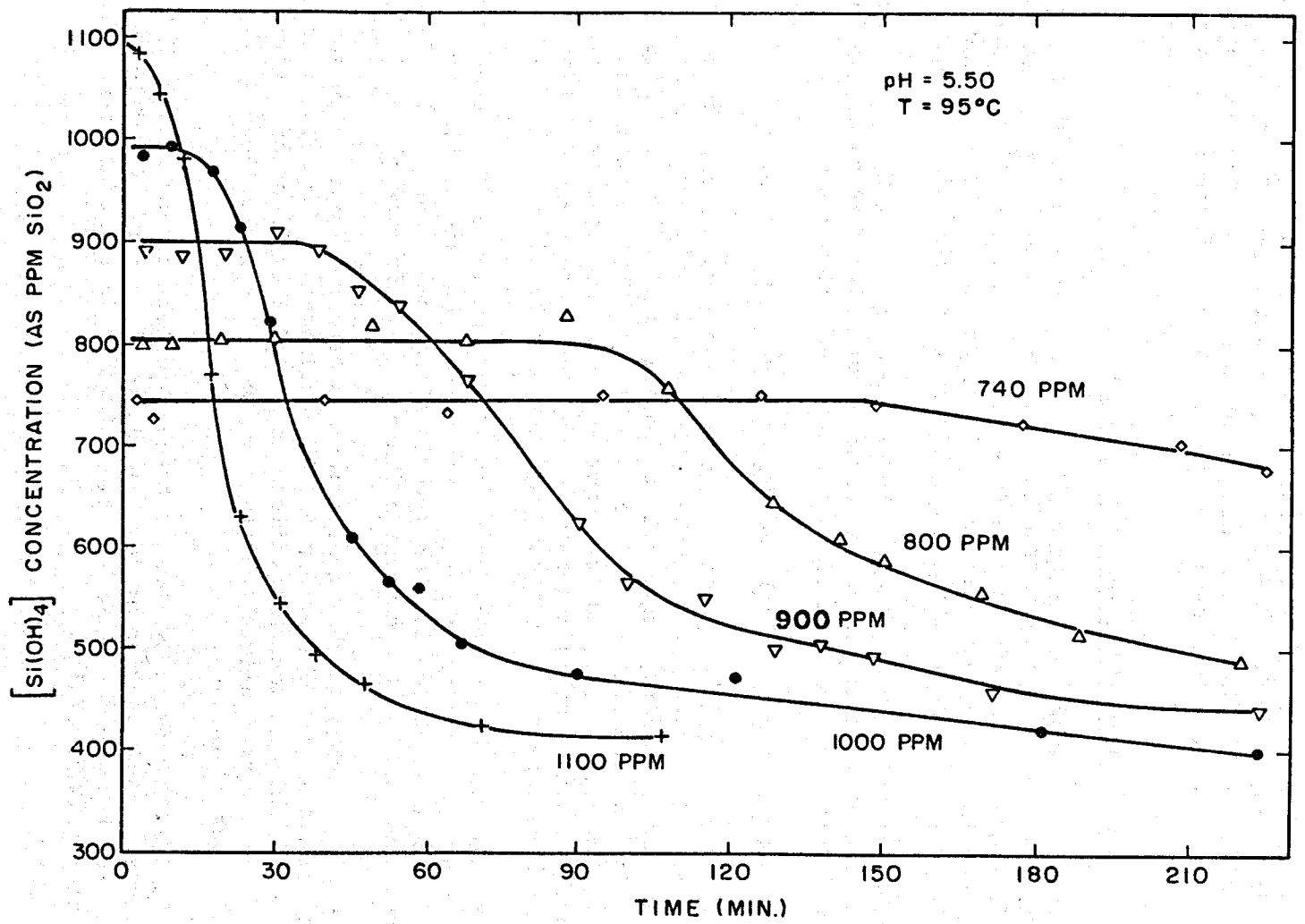

Fig. 7: Silica condensation as a function of time for a series of initial silicic acid concentrations.

6. Condensation Kinetics at pH 5.50 and Various Temperatures

The rate of condensation in the standard brine at a fixed, initial silicic acid concentration of 900 ppm as SiO_2 was determined at temperatures from 75° to 105°C. Results are given in Figure 8. The comments made previously on the temperature dependence at pH 4.50 apply at pH 5.50 also.

7. Condensation Kinetics at pH = 6.50 and 95°C

The HAc/Ac system has little buffering capacity above pH of about 5.50; accordingly, a maleate buffer was used at pH 6.50. Results in the two buffers at pH 5.50 are compared in Figure 9. There is little difference between the two solutions. The small differences evident in the figure are due to a small difference in initial silicic acid concentration.

The rate of condensation in the standard brine at pH 6.50 is shown as a function of initial concentration in Figure 10. Results are analogous to those obtained at lower pH's, except that the rates are higher.

8. Observations of Light Scattering during Condensation

The extent of light scattering by solutions undergoing condensation was determined (in parallel with the silicic acid analyses) at a wavelength of 400 nm in a 1-cm path length cell thermostated at 25°C. An aliquot of the solution was acidified, a portion of the acidified solution was introduced into the cell, and its apparent absorbance measured. Absorbances were then calculated by taking into account the appropriate dilution factors. Results for various runs are shown in Figures 11 to 13.

Results in Figure 11 refer to pH = 4.50 and T = 95°C. Absorbances are plotted as a function of extent of reaction for each initial concentration. Extent of reaction is simply the difference between C_o, the initial concentration, and C_t, the concentration at any later time t.

Figures 11 and 12 show that solutions with relatively high initial concentrations do not scatter appreciably until the condensation reaction is far advanced; solutions more dilute in silicic acid scatter light earlier, and the most dilute solutions begin to scatter as soon as the transition period is over.

Figure 13 shows a systematic trend of extent of scattering with temperature. Condensation at 105°C leads to scattering at smaller values of extent of reaction than condensation at 75°C; intermediate temperatures yield intermediate results.

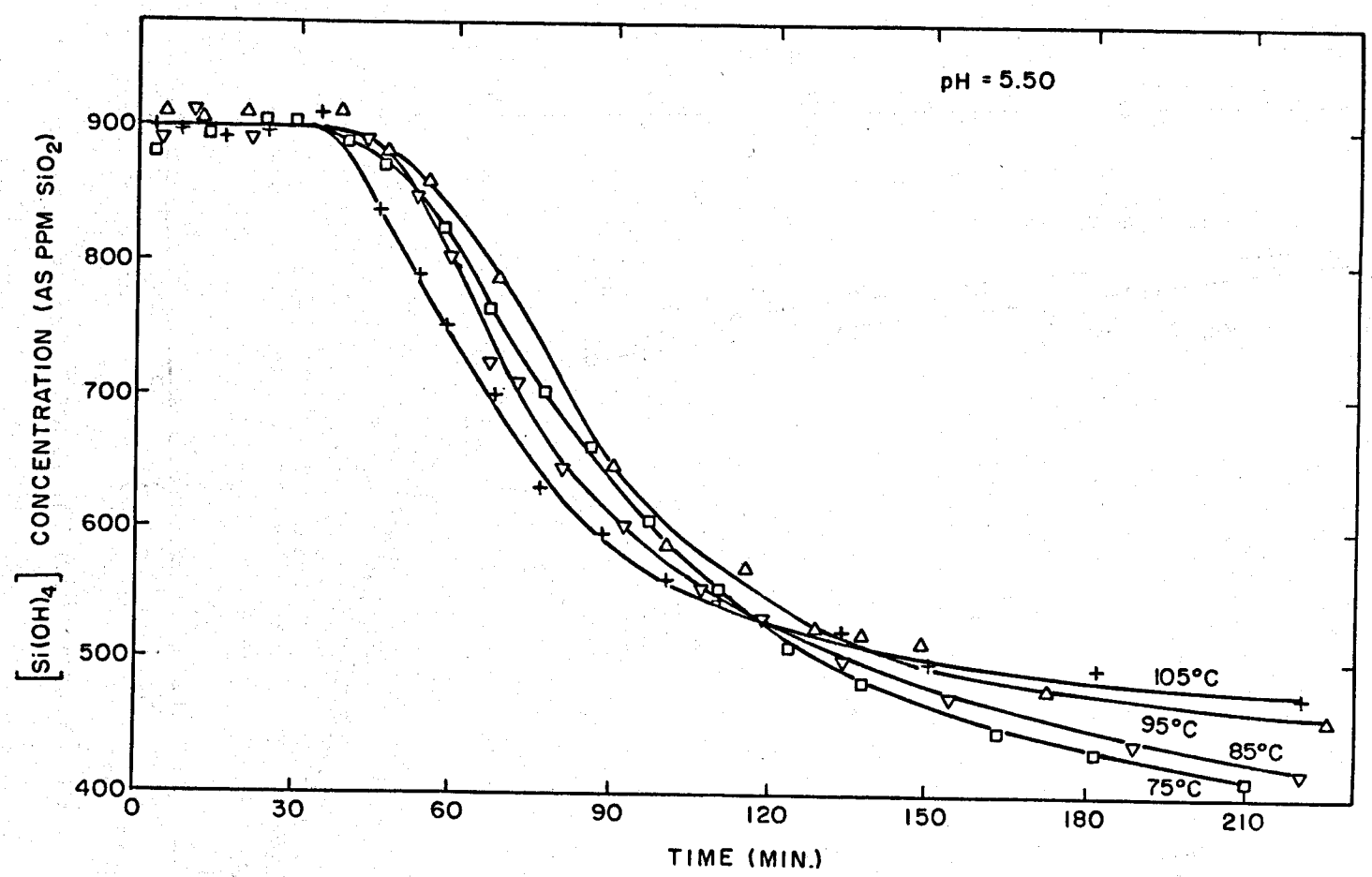

Fig. 8: Silica condensation from a solution of 900 ppm (as SiO_2) initial concentration as a function of time at various temperatures.

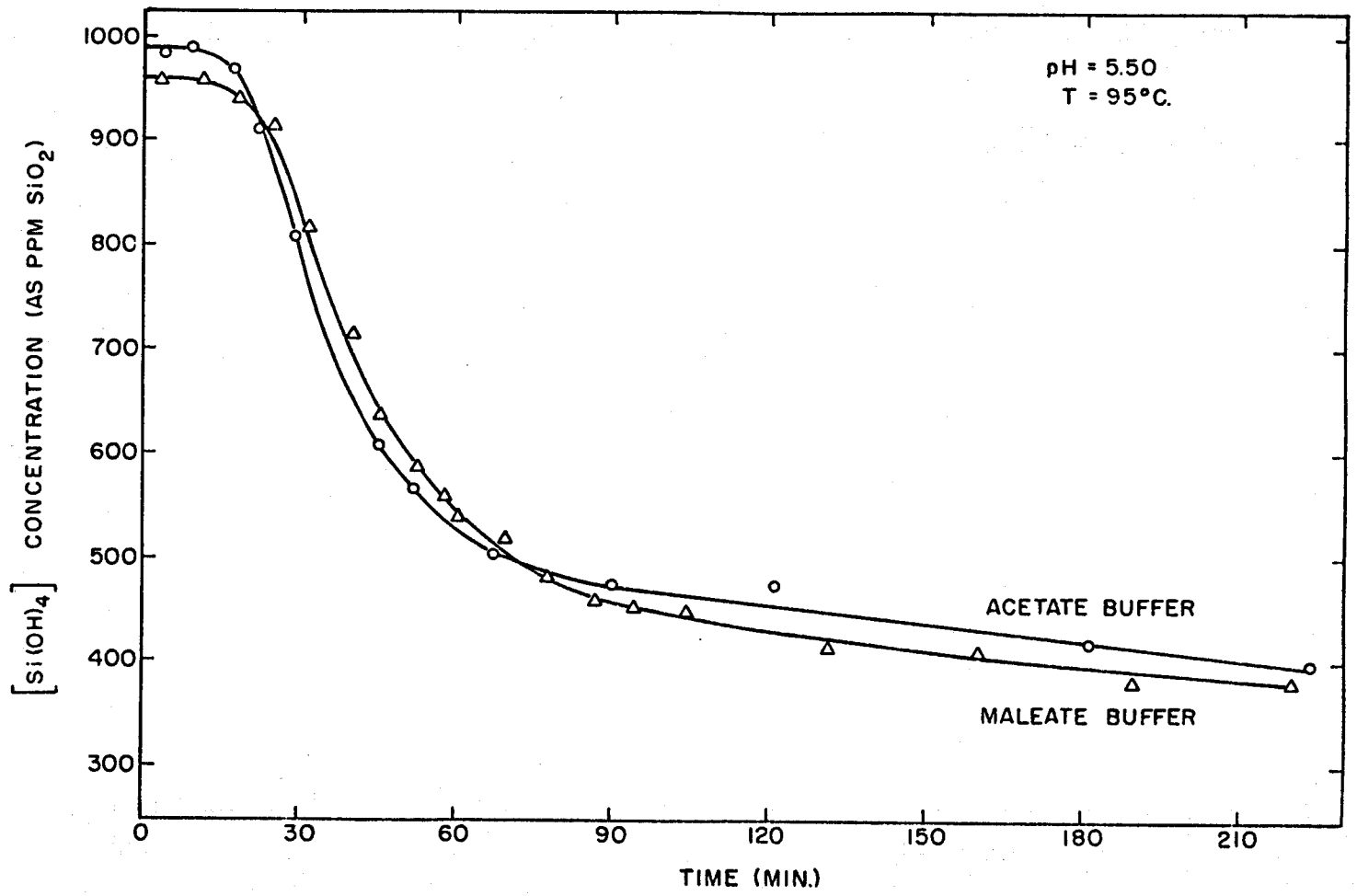

Fig. 9: Silica condensation as a function of time at pH 5.50 in acetate and maleate buffers.

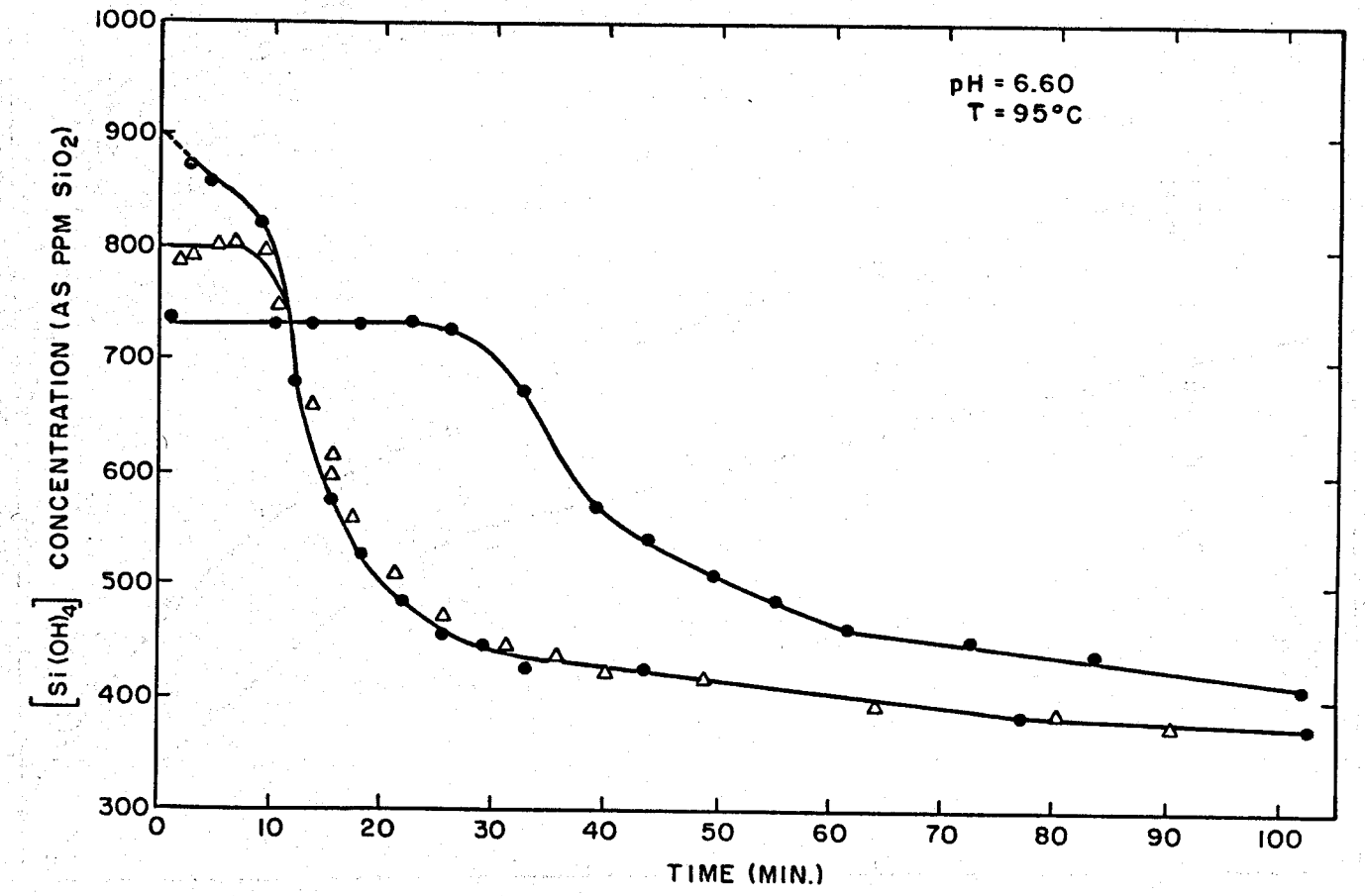

Fig. 10: Silica condensation as a function of time for a series of initial silicic acid concentrations.

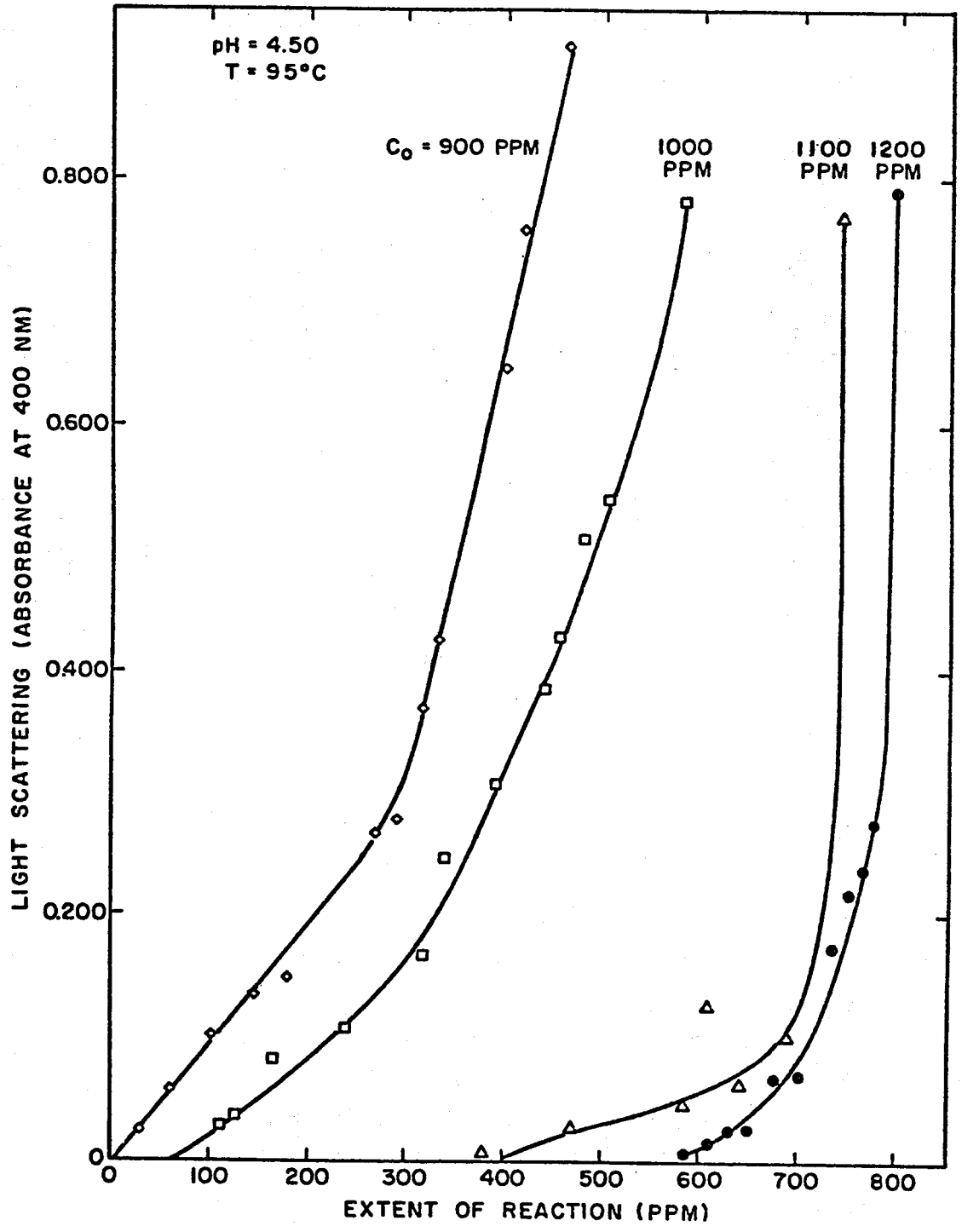

Fig. 11: Light scattering by acidified aliquots of solutions during condensation.

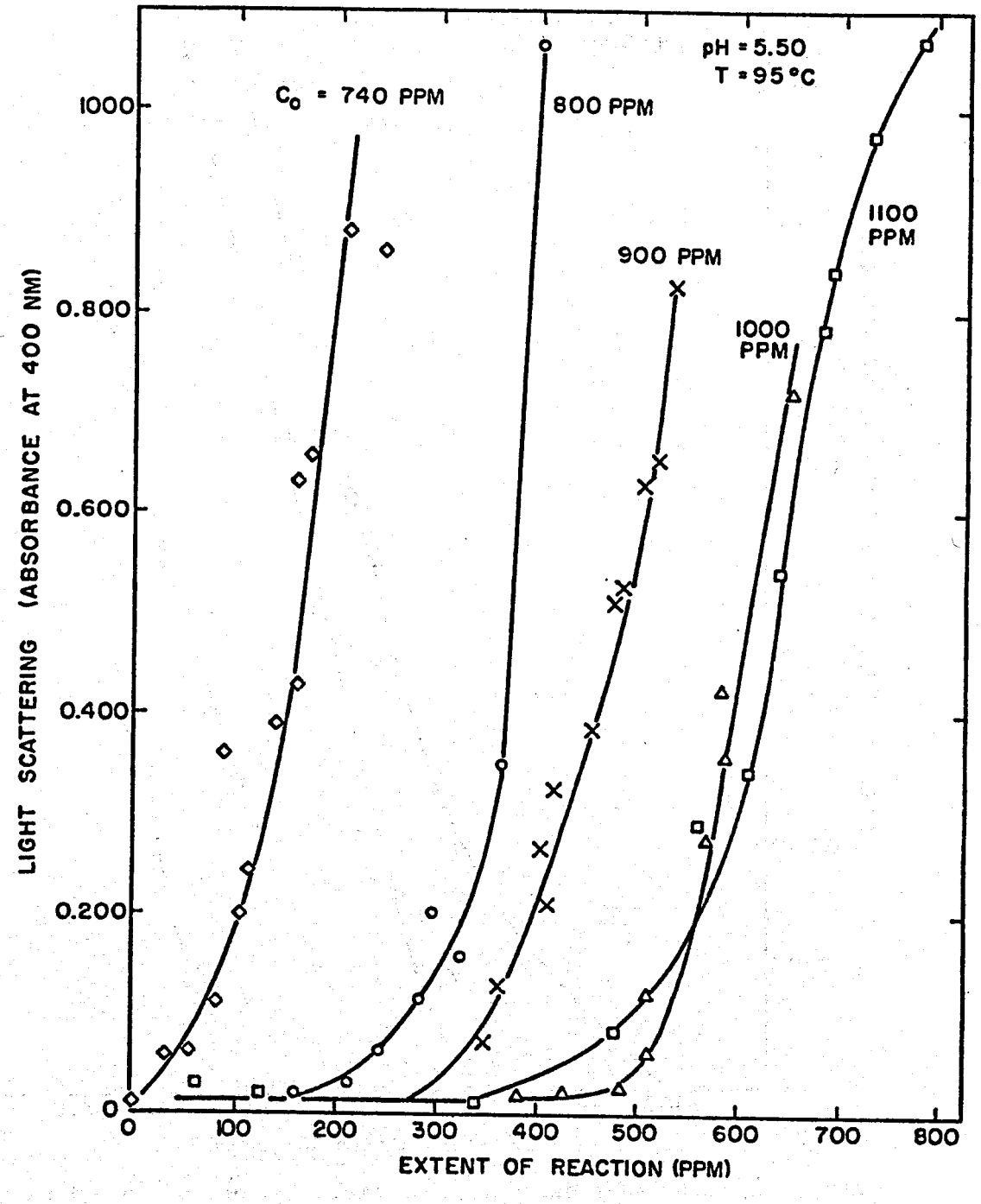

Fig. 12: Light scattering by acidified aliquots of solutions during condensation.

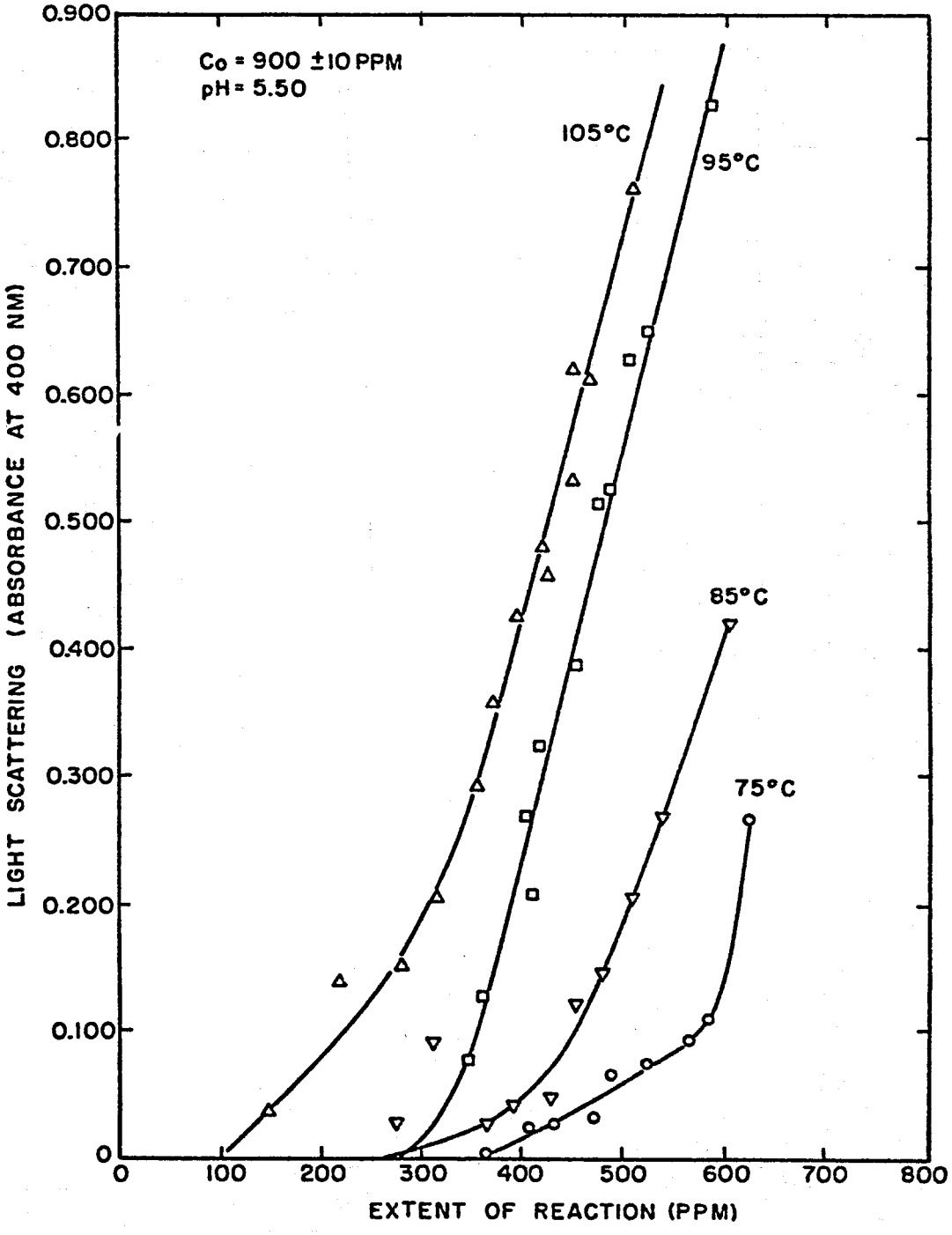

Fig. 13: Light scattering by acidified aliquots of solutions during condensation at a fixed initial concentration (900 ppm as SiO_2) and a series of condensation temperatures.

IV. DISCUSSION

1. Introduction

Kinetics of condensation (precipitation) of SiO_2 from relatively dilute solutions of silicic acid have been reported by a number of authors (2,6-12). There is general agreement that the rate depends strongly on pH (6-10). Below pH 3, the reaction at room temperature appears to be catalyzed by H^+, and the rate is approximately ten times faster at pH 1 than at pH 2. Between pH 3 and pH 6, the reaction rate depends on OH^- and is approximately 100 times faster at pH 6 than at pH 4. The rate of disappearance of monomer is at a minimum near pH 3. Between pH 7 and pH 10, the reaction rate increases by a factor of about 3.4 for each unit increase in pH (7).

Results between pH 3 and pH 6 are consistent with a reaction mechanism, proposed by Ashley and Innes (9,10), involving reaction of ionized and non-ionized silicic acid species. This mechanism predicts that the reaction rate should decrease by a factor of ten for each unit decrease in pH below about pH 9. The first pK_a for monomeric silicic acid at room temperature is about 9.8 (11-13); the corresponding pK_a for oligomeric silicic acids is in the range 9.5-10.7 (14).

In the pH range 7-10, Okamoto and co-workers (7) find the reaction at room temperature to be third order with respect to "molecularly dispersed" silica and to follow a rate law

$$-\frac{dC}{dt} = k(C-S)^3 \qquad (1)$$

where C is the concentration of monomeric silica and S the equilibrium solubility of monomer. The same rate law was found by Jorgensen (15) in 1M $NaClO_4$ of pH between 4 and 5, and this rate law was also found for dissolution of silica gel. However, since the pH was not controlled (the solution was unbuffered), these data (15) are of limited quantitative value.

More recently, Bishop and Bear (16) have reported that the rate of disappearance of monomer is second order with respect to monomer at pH 8.5. This order is somewhat doubtful, however, since it was difficult to fit this rate law at both the beginning and the end of the reaction. On the other hand, Alexander (17) also reports what may be a second order rate law at pH 4.4, and this is confirmed by Kitahara (2). Kitahara reports the reaction to be third order with respect to monomer at higher pH.

In contrast to reported second- and third-order kinetics, Coudurier and co-workers (6) find the reaction rate to be first order at pH 7.2. At pH 2, however, the reaction appeared to be second order, and the authors propose a reaction order between 1 and 2 for intermediate pH's. The rate equation used to summarize their data at pH 4 is

$$-\frac{dC}{dt} = k[C]^{1.84} \exp\,(0.135[P]) \qquad (2)$$

where [P] is the total concentration of oligomeric and polymeric silicic acids and [C] is the total concentration of monomer and dimer, both in grams/liter. The origin of the exponential term is not clear, although the strong dependence on polymeric silica implies some sort of auto-catalytic mechanism. In any event, the silicic acid used in the study by Coudurier et al. was prepared as a mixture of monomer, dimer, and oligomer, with the major fraction in dimeric form.

Results obtained by Baumann (18) are different from those discussed above. Baumann found that at low initial concentrations of silicic acid (less than 500 to 1000 ppm, depending on pH which was varied from 0.5 to 9.0), the initial rate of disappearance of monomer was essentially zero. After an induction period ranging from a few minutes to an hour, the reaction rate increased, reached a maximum value, and then decreased again toward zero as the equilibrium value of the silicic acid solubility was approached. The apparent reaction order with respect to monomer concentration varied from first order to fifth order at a given pH. In a subsequent paper (18), Baumann reported that oligomers produced at pH 3 depolymerized when the solution was diluted and the pH raised to 6.1, but then condensed again with time.

Induction periods for the condensation of monomeric silica from natural geothermal brines have also been reported (19).

The effect of temperature on the rate of condensation of silicic acid has been studied by a number of investigators. Coudurier and co-workers (6) find an activation energy of about 15 kcal/mole in the vicinity of pH 4, for temperatures between 20° and 60°C. In the same temperature and pH range, Stade and Wieker (8) find nearly the same activation energy for the dissolution reaction, although they find that the activation energy appears to vary with pH outside of this range. In Kitahara's study (2), an activation energy of 10 kcal/mole was found at pH 6.

In sharp contrast to these results, Bishop and Bear (16) found that between 25°C and 35°C at pH 8.5 the reaction rate first decreased with increasing temperature, and then increased above 35°C. Their "activation" energy is -16 kcal/mole between 35°C and +14 kcal/mole above.

The condensation of silicic acid has been studied by other methods in addition to measurement of the rate of disappearance of molybdate-reactive, dissolved species. Experimental approaches include measurement of the time required for gel formation (20) and, more quantitatively, changes in viscosity (21-23) and light scattering (6,10,21-23) with time. Other methods include ultracentrifugation (21) for obtaining the molecular weight distribution, and chromatography (24), to estimate the concentrations of various oligomers. Most of these methods are only applicable to solutions that have condensed to some extent. For example, Coudurier and co-workers (6) have shown that light scattering is not observed at pH 5 until after 80% of the starting material has condensed.

2. Theory of Condensation Reactions in Solution

If we consider the results obtained here and by others in their totality, it becomes apparent that it is not possible to arrive at a purely chemical mechanism for condensation (precipitation) of SiO_2 from silicic acid solutions. A correct description of the process must be based on the theory of condensation and phase transitions.

A transition between a supersaturated, homogeneous solution and a two-phase, equilibrium system involves a change in free energy given by

$$-\Delta G = RT \ln \frac{a}{a_e} \approx RT \ln \frac{C_o}{C_e} \qquad (3)$$

where a is the activity of the solute in the supersaturated solution and a_e that for a saturated solution. Although the free energy difference between initial (supersaturated) and final (equilibrium) states is negative, the free energy may increase in the initial stages of condensation because of contributions from interfacial free energy as nuclei are formed. The situation is conventionally described by assigning volume free energies to the bulk phases and a surface free energy to the interface region; for sufficiently small particles of the solid phase, the surface term is dominant.

In general, volume changes associated with nucleation of a solid phase may produce a disordered solid phase. Each particle (nucleus) may be, therefore, a source of internal stress which contributes to the overall free energy change of the assembly. In the particular case of SiO_2, the solid phase that nucleates is largely amorphous, though its structure, and to some extent, chemical composition, particularly H_2O content, may depend on the conditions of condensation.

Neglecting strain energies, we may treat the transition region between solution and solid as a geometrical surface with a specific interfacial free energy γ_{SL} per unit area. A particle (nucleus) with

radius r (assuming spherical particles), is in equilibrium with a supersaturated solution when

$$\ln \frac{C}{C_e} = \frac{2\gamma_{SL} v_S}{r\ kT} \tag{4}$$

where v_S is the molecular volume of the solid phase and the other symbols have their usual significance. For any degree of supersaturation, the equilibrium between particles having radius r and a solution of concentration C is unstable, since such a solution is unsaturated with respect to smaller and supersaturated with respect to larger particles. The instability of equilibrium is expressed in a formal way by a maximum (rather than a minimum) of the free energy of the system at some value $r = r_c$. The maximum is

$$\Delta G'_{max} = \frac{4\pi}{3} (r_c)^2 \gamma_{SL} \tag{5}$$

A generalized theory of condensation based on the assumption that even in the range of thermodynamic stability of a phase A, fluctuations lead to a certain distribution of embryos of phase B, was first developed by Volmer (25). Kinetic expressions were derived by neglecting embryos markedly exceeding the critical size r_c corresponding to $\Delta G'_{max}$. A more general expression was subsequently developed by Becker and Doring (26) who solved the system of differential equations involving the rates of formation of nuclei of various sizes. The general equation is

$$\frac{\partial Nn}{\partial t} = I_n - I_{n+1} \tag{6}$$

where N_n is the number of particles containing n molecules, I_n is the number of particles which pass from class n-1 to class n per unit time, and I_{n+1} the corresponding quantity for transitions from class n to n+1. This equation can be solved assuming that the rate of formation of embryos of size n is small and essentially independent of time (quasi-steady-state distribution) and that the number of molecules in particles is small compared to the total number of molecules in solution.

The nucleation rate per unit volume is

$$I = N \frac{kT}{h} \frac{O_c}{n_c} \left(\frac{\Delta G_c}{3\pi kT}\right)^{1/2} \exp\left(-\frac{\Delta G_c + \Delta_\alpha g^\dagger}{kT}\right) \tag{7}$$

where N is the number of molecules per unit volume, kT/h is a frequency factor, O_c/n_c is the ratio of surface atoms to total atoms in a critical size embryo, and $\Delta_\alpha g^\dagger$ is the activation energy for transfer of a molecule

from solution to the surface. ΔG_c, the free energy change corresponding to formation of embryos of critical size (containing n_c molecules), is given by

$$\Delta G_c = \Delta G_c' + kT \ln(Q_{tr}Q_{rot}/Q_{rep}) \tag{8}$$

where $\Delta G_c'$ is

$$\Delta G_c' = \frac{4\pi r_c^2 \gamma_{SL}}{3} \tag{9}$$

and Q_{tr}, Q_{rot} and Q_{rep} are partition functions corresponding to translational, rotational and "replacement" contributions to the energy of the system upon formation of embryos. When both phases are condensed, it is likely that these contributions are relatively small, so that

$$\Delta G_c \simeq \Delta G_c' = \frac{4\pi r_c^2 \gamma_{SL}}{3} \tag{10}$$

Also, the quantity $O_c/n_c(\Delta G_c/3\pi kT)^{1/2}$ is within one or two powers of ten, so that Eq. (7) may be written with sufficient accuracy as

$$I = N \frac{kT}{h} \exp\left(-\frac{\Delta G_c + \Delta \alpha g^{\ddagger}}{kT}\right) \tag{11}$$

3. The Transition Period

A detailed discussion of condensation kinetics in the initial stages (where the concentration is little changed from the initial concentration, C_o) is given in Appendix C. An apparent transition period is observed at the beginning of the condensation process. During this period, the rate of removal of material from solution is below the detection limit of the analytical technique used to determine silicic acid in solution. The analysis given in Appendix C shows that at a fixed pH the transition period, τ', is related to supersaturation by:

$$\ln \tau' = -\frac{3}{4} \ln (C_o - C_e) + \frac{\beta/4}{(\ln C_o/C_e)^2} + \text{Constant} \tag{8}$$

where C_o is the initial concentration, C_e the equilibrium concentration, and β a constant related to the activation energy for nucleation. When $C_o \gtrsim 3C_e$, the first term on the right can be neglected, and $\ln \tau'$ varies as $1/(\ln C_o/C_e)^2$.

4. Activation Energy for Silica Precipitation

The temperature coefficient was determined at a fixed salinity and concentration of silicic acid at two pH values (4.50 and 5.50). In both cases, the transition period, τ', is essentially the same in the temperature interval 75°-105°C and the rates at times greater than τ' are only slightly affected by temperature. These results suggest that to a first approximation, the condensation rate is nearly independent of temperature. Apparently, the increase in rate brought about by the exponential dependence of the nucleation rate and of the specific rate constant on (1/T) is essentially counterbalanced by a decrease in rate brought about by decreased supersaturation (larger C_e) at higher temperatures.

An analysis of the temperature dependence and of activation energies is given in Appendix D. From these results and the value of the heat of solution of SiO_2 (2.65×10^3 cal/mol), we can show that

$$\Delta_\alpha g^\dagger \simeq \Delta G_c \qquad (12)$$

with these terms already defined in connection with Eq. (11) above.

Furthermore, using $\gamma_{SL} = 45$ ergs/cm^2, a value estimated from variations in solubility with particle size (27) and consistent with the analysis of $\ln(\tau')$ vs. $1/[\ln(C_o/C_e)]^2$ plots given in Appendix C, we have

$$\Delta G_c = 11.9 \times 10^{-20} \text{ joule}$$

and $$\Delta_\alpha g^\dagger = 17 \text{ kcal/mol per mole of silicic acid}$$

Thus, the condensation process is highly activated during nucleation and growth.

5. The pH Dependence of Condensation Kinetics

The pH dependence of the transition period demonstrates clearly the large effect of pH on condensation kinetics. As is evident in the discussion of growth kinetics (see below), the pH dependence of the overall kinetics is more complicated because it reflects effects arising both during nucleation and growth.

Transition times decrease by approximately a factor of 10 for each pH increase in the range of pH 4.50 to 6.50. The increase in reaction rate brought about by increasing pH may be viewed as catalysis by OH^- or simply as evidence that the reacting species is the singly ionized $SiO(OH)_3^-$ molecule. The simple hypothesis that the reacting species is

$SiO(OH)_3^-$ seems to be adequate for describing the pH dependence. The concentration of $SiO(OH)_3^-$ is

$$[SiO(OH)_3^-] = \frac{K_1 [Si(OH)_4]}{[H^+]} \tag{13}$$

where K_1 is the first ionization constant of $Si(OH)_4$. Its value in solutions of low ionic strength at 95°C is estimated as $10^{-9.8}$. Accordingly,

$$[SiO(OH)_3^-] \simeq 5 \times 10^{-6} \; [Si(OH)_4] \text{ at pH} = 4.50$$

and

$$\simeq 5 \times 10^{-4} \; [Si(OH)_4] \text{ at pH} = 6.50$$

Since, as shown below, the nucleation rate is directly proportional to the concentration of reacting species, the transition time is expected to decrease by about a factor of 10 for each pH unit increase in this range.

6. Condensation Kinetics - Nucleation

The discussion above may be summarized by writing for the nucleation rate per unit volume

$$I = N \frac{kT}{h} \exp(-2\Delta G_c/kT) \tag{14}$$

where

$$\Delta G_c \simeq \frac{4}{3} \pi r_c^2 \gamma_{SL} \tag{15}$$

with γ_{SL} the interfacial energy between amorphous silica and solution and r_c the radius of the critical size nucleus. The radius of the critical size nucleus is given by

$$r_c = \frac{2\gamma_{SL} v_S}{kT \ln(C_o/C_e)} \tag{16}$$

with v_S the volume of a molecule of silica in the solid phase ($v_S \simeq 4.5 \times 10^{-23}$ cm^3). The value of γ_{SL} is estimated at 45 ergs/cm^2 from the variation of solubility with particle size (27). This value gives approximately a correct order of magnitude for the observed condensation kinetics (nucleation rates). Using these values of v_S and γ_{SL} we find at $C_o/C_e \simeq 2.7$ or $\ln C_o/C_e \simeq 1$, that

$$r_c \simeq 8 \times 10^{-8} \text{ cm} \tag{17}$$

and

$$n_c = \frac{4}{3} \pi (r_c)^3 / v_S \simeq 45 \text{ molecules} \tag{18}$$

where n_c is the number of silica molecules in a nucleus of critical size.

The energy of activation is given by

$$\Delta G_c = \frac{16}{3}\pi\left(\frac{v_S}{kT}\right)^2 \gamma_{SL}{}^3 = 11.9 \times 10^{-20} \text{ joule} \qquad (18)$$

$$\Delta_\alpha g^\dagger \simeq \Delta G_c \qquad (19)$$

and

$$\frac{\Delta G_c}{kT} \simeq 23 \qquad (20)$$

The rate of nucleation can be estimated from these values by using Eq. (7). In the pre-exponential term, $N \simeq 1 \times 10^{19}$ molecules/cm^3 and $kT/h \simeq 10^{13}$. Using as an example specific conditions applicable at pH = 4.50 and $C_o/C_e = 2.73$ or $\ln C_o/C_e \simeq 1$, and assuming that the reacting entity is $SiO(OH)_3^-$, we have

$$I \simeq (5 \times 10^{-6})(10^{19})(10^{13})\exp(-46) \simeq 5 \times 10^6 \text{ nuclei per sec per cc}$$

The reaction volume was 125 cc and the transition period under these conditions (C_o ~1000 ppm as SiO_2) about 200 min. The number of nuclei formed is thus about 10^{13} to 10^{14}. This number of nuclei eventually accounts for the removal of about 10^{21} molecules of silicic acid from solution. Accordingly, precipitated particles eventually contain about 10^8 molecules of silicic acid and have a radius in the range of 1000 Å These estimates yield a reasonable description of the precipitation process within the range of experimental observations. Agreement within a few orders of magnitude is characteristic of the description of condensation phenomena from general kinetic theory (28).

7. Condensation Kinetics - Growth

Kinetics of growth are expected to be initially controlled by the rate of addition of molecules (or ions) of silicic acid to nucleated particles; at some later time, diffusional limitations may set in. "Ripening" of the precipitate, that is, dissolution of small particles and continued growth of the larger ones, will also take place.

The interpretation of kinetic curves, i.e., of C vs. t plots, is complicated by several factors. We note first that as the reaction proceeds, the nucleation rate decreases as $\exp -\{1/[\ln(C/C_e)]^2\}$. Thus, the rate of nuclei formation is appreciable even after the concentration has decreased to, say, half its original value. However, the amount of SiO_2 involved in the formation of nuclei of critical size is negligible

as a simple calculation will show. For all practical purposes, the observed decrease in concentration may be exclusively associated with particle growth.

We have given in Appendix C an analysis of the initial kinetics and of the dependence of the transition time on initial supersaturation. The derived rate expressions are in good agreement with observed kinetics, at least for pH = 4.50. For later stages of the reaction, the apparent dependence of C on time is approximately linear over a fairly wide range of initial supersaturations, but the slope decreases with decreasing C_o. This apparent regularity is to some extent misleading, since the average particle size for the same extent of reaction is widely different for different initial concentrations. Qualitatively, this variation in average particle size is shown by observations of light scattering at various stages of reaction. These observations are discussed below.

8. Light Scattering

Apparent absorbances were shown as a function of extent of reaction (i.e., of C_o-C) in Figures 11-13. It is evident from Figures 11 and 12 (pH = 4.50 and 5.50) that the dependence of "absorbance" on extent of reaction is different for different supersaturations. At large supersaturations, little or no scattering is observed until the condensation reaction is essentially over; that is, until C has decreased almost to its equilibrium value. On the other hand, at lower supersaturations scattering is observed essentially as soon as the concentration changes significantly from its initial value. An interpretation of the course of condensation consistent with these facts is that the average particle size in solutions with large initial supersaturations is too small to lead to scattering, at least up to the point where considerable ripening of the solution has occurred. On the other hand, particle sizes in less supersaturated solutions are, on average, larger for the same extent of reaction. Consequently, scattering is observed much earlier in the course of reaction.

Figure 13 presents results for light scattering at different temperatures of condensation. It is of interest that results with solutions of fixed initial concentration (900 ppm as SiO_2 at pH = 5.50) but varying temperatures (T = 75° to 105°C) are consistent with what is expected on the basis of decreased supersaturation as the temperature is raised. Light scattering during condensation at 75°C (low C_e hence high C_o/C_e at fixed C_o) has characteristics of solutions of relatively high supersaturation while light scattering during condensation at 105°C follows the pattern of less supersaturated solutions. Results at 85° and 95°C are intermediate. These observations support in a qualitative fashion our analysis of the temperature dependence of the condensation reaction given in Appendix D.

9. Effects of Other Solution Species

The effect of salinity on condensation rate follows what is expected from a decrease in equilibrium concentration of silicic acid as the salt concentration increases (Figure 4). For example, the transition time at pH = 4.50 decreases regularly with increasing salt concentration at a fixed, initial silicic acid concentration. The analysis given in Appendix C shows that the values of τ' are what are expected for the corresponding C_o/C_e values. Accordingly, we may conclude that there are no specific effects on rate by NaCl and KCl.

Additions of $CaCl_2$ or $MgCl_2$ to the brine do not affect the rate. The compositions of the solutions are given in Table 1 and the kinetic results in Figure 14.

Addition of NaF has a significant effect on the condensation rate. Solution compositions are given in Table 2 and kinetic results are shown in Figure 15. It is clear that fluoride ion in small concentrations accelerates substantially the rate of condensation.

The mechanism of this effect was not established, but it is clear from Table 2 that F^- displaces OH^- from $Si(OH)_4$. This is shown by the larger quantity of HAc needed to achieve the final pH = 4.50 as NaF is added to solution. Evidently, the fluoride-containing silica species are more reactive than silicic acid itself.

Table 1

Solution Compositions at pH = 4.50

	Standard Brine (M)	Brine with Calcium (M)	Brine with Magnesium (M)
Na^+	0.452	0.353	0.353
K^+	0.065	0.065	0.065
Cl^-	0.315	0.315	0.315
Ac^-	0.202	0.202	0.203
HAc	0.205	0.205	0.204
Ca^{++}	-	0.050	-
Mg^{++}	-	-	0.050

Table 2

Make-up of Solutions Containing NaF
(Total Volume 125 cc)

	Standard Brine (mmoles)	Solution 1 (mmoles)	Solution 2 (mmoles)	Solution 3 (mmoles)
$Na_2H_2SiO_4$	17.380	17.380	17.380	17.380
NaCl	12.369	12.243	12.054	11.739
NaF	-	0.126	0.315	0.630
KCl	8.127	8.127	8.127	8.127
HCl	18.879	18.879	18.879	18.879
NaAc	26.691	26.691	26.691	26.691
HAc	24.150	24.570	25.200	26.460

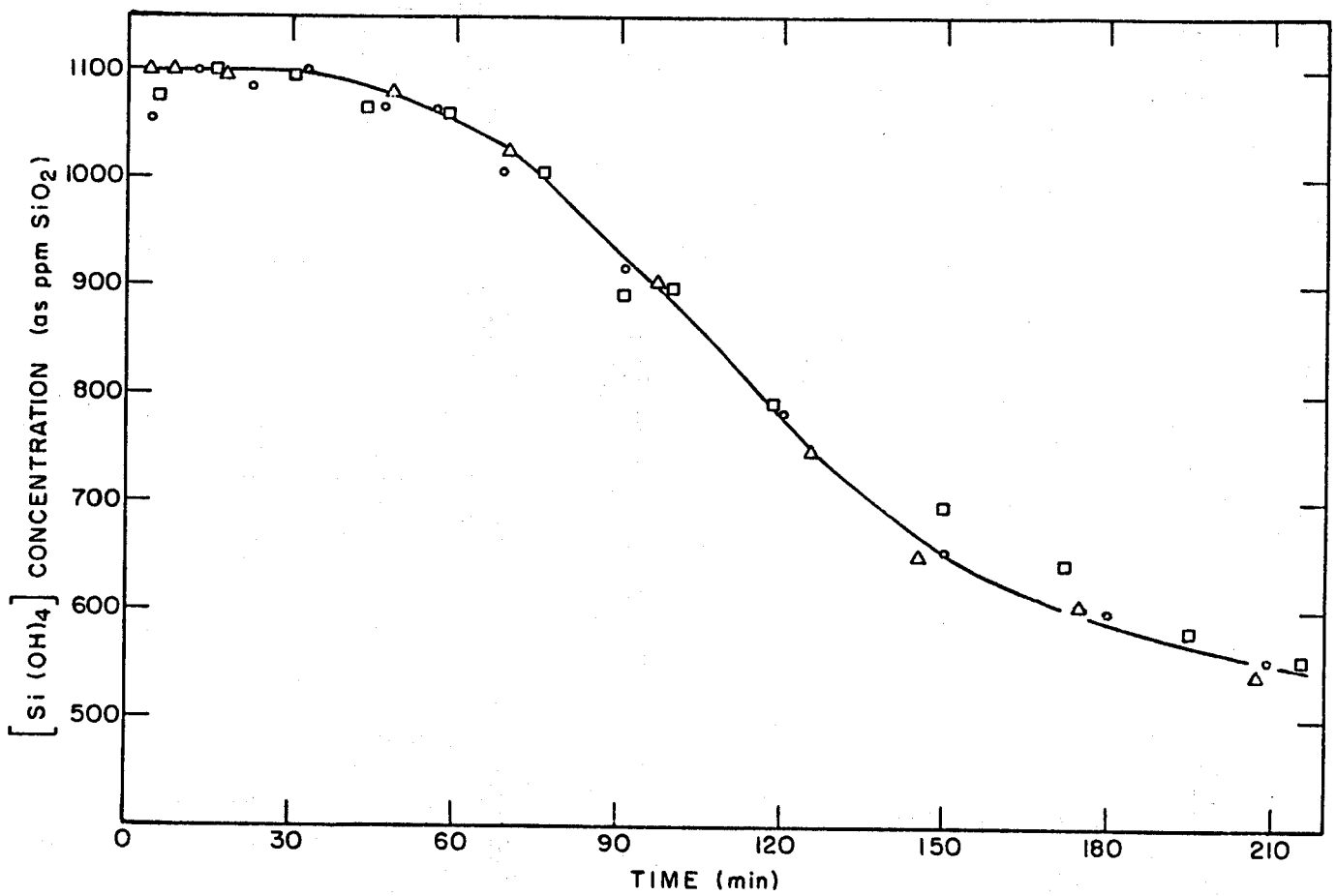

Fig. 14: Effect of additions of Ca^{++} (o) and Mg^{++} (□) on kinetics in standard brine (Δ).

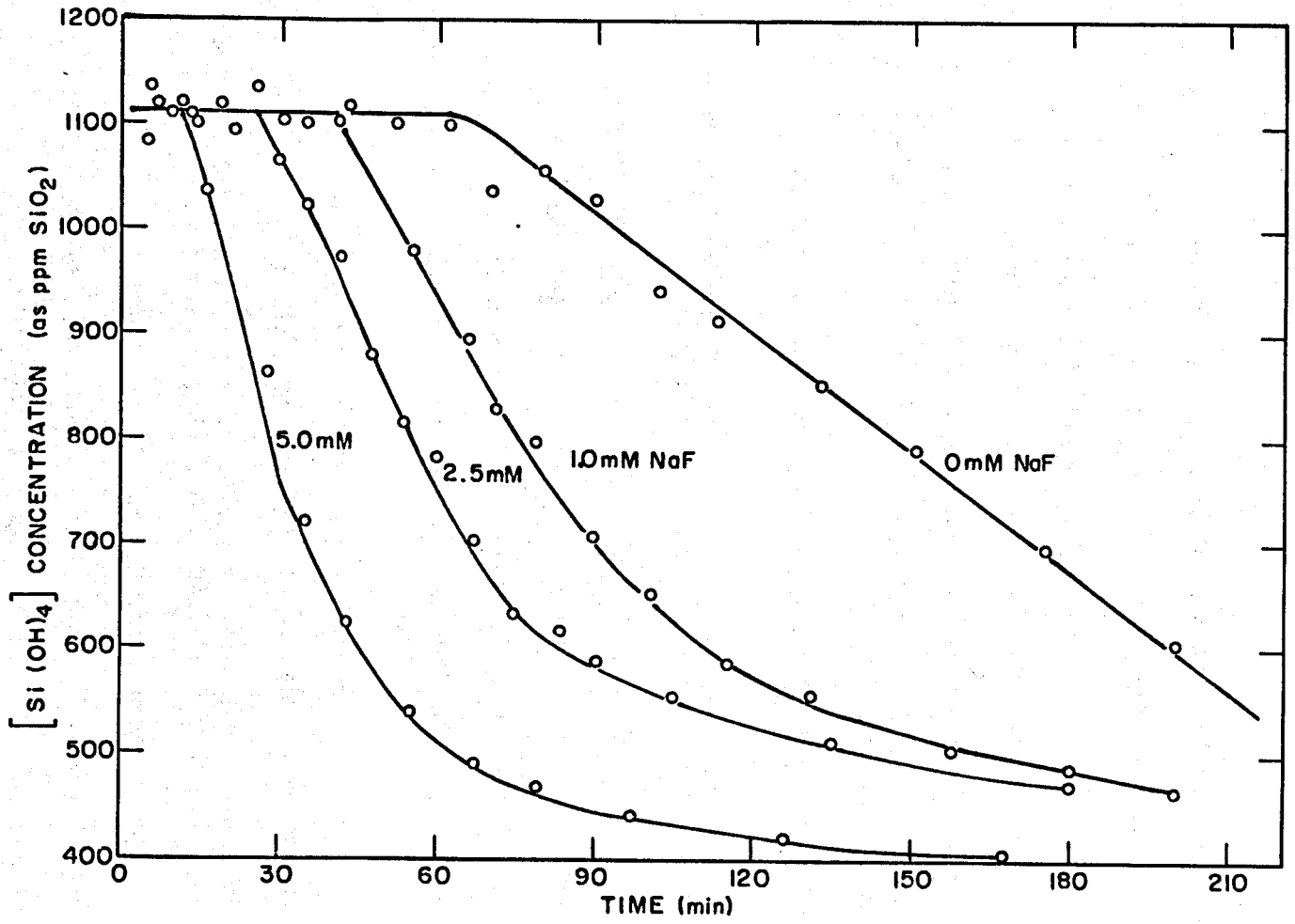

Fig. 15: Effect of NaF additions on condensation rate of silicic acid.

V. REFERENCES

1. D. F. Weill and Y. Bottinga, Contr. Mineral. Petrol. 25, 125 (1970).

2. S. Kitahara, Rev. Phys. Chem. Japan 30, 131 (1960).

3. V. W. Truesdale and C. J. Smith, Analyst 100, 203 (1975).

4. G. B. Alexander, J. Am. Chem. Soc. 75, 5655 (1953).

5. A. R. Marsh, G. Klein and T. Vermeulen, "Polymerization Kinetics and Equilibria of Silicic Acid in Aqueous Systems," Final Report, ERDA Contract W-7405-ENG-48, Published as LBL-4415, Univ. of California, Berkeley, October 1975.

6. M. Coudurier, B. Baudru and J. B. Donnet, Bull. Soc. Chim. France, 3147, 3154, 3161 (1971).

7. K. Goto, J. Phys. Chem., 60, 1007 (1956); G. Okamoto, T. Okura and K. Goto, Geochim. Cosmochim. Acta 12, 123 (1957).

8. H. Stade and W. Wieker, Z. anorg. allg. Chem. 384, 53 (1971).

9. K. D. Ashley and W. B. Innes, Ind. Eng. Chem. 44, 2857 (1952).

10. S. A. Greenberg and D. Sinclair, J. Phys. Chem. 59, 435 (1955).

11. A. G. Volosov, I. L. Khodakovskiy and B. N. Ryzhenko, Geochemistry International, 362 (1972).

12. T. M. Seward, Geochim. Cosmochim. Acta 38, 1651 (1974).

13. H. Bilinski and N. Ingri, Acta Chem. Scand. 21, 2503 (1967).

14. V. N. Belyakov, N. M. Soltirskii, D. N. Strazhenko and V. V. Strelko, Ukrainskii Khimcheskii Zh. 40, 236 (1974).

15. S. S. Jorgensen, Acta Chem. Scand. 22, 335 (1968).

16. A. D. Bishop and J. L. Bear, Thermochimica Acta 3, 399 (1972).

17. G. B. Alexander, J. Am. Chem. Soc. 76, 2094 (1954).

18. H. Baumann, Koll. Zeit. 162, 28 (1959); Z. Anal. Chem. 217, 241 (1966).

19. D. E. White, W. W. Brannock and K. J. Murata, Geochim. Cosmochim. Acta 10, 27 (1956).

20. S. P. Moulik and D. K. Mullick, J. Polymer. Sci. 4-A1, 811 (1966).

21. A. Audsley and J. Aveston, J. Chem. Soc., 2320 (1962).

22. B. G. Linsen, J. H. deBoer and C. Okkerse, Rev. Trav. Chim. 79, 439 (1960).

23. S. P. Moulick, B. N. Gosh and S. Bandyopadhyay, J. Ind. Chem. Soc. 40, 607 (1963).

24. D. Hoebbel and W. Wieker, Z. anorg. allg. Chem. 400, 148 (1973); 366, 139 (1969); 400, 148 (1973).

25. M. Volmer and A. Weber, Z. Physik. Chem. 119, 277 (1926); M. Volmer, Z. Elektrochem. 35, 555 (1929); M. Volmer and H. Flood, Z. Phys. Chem. 170A, 273 (1934).

26. R. Becker and W. Doring, Ann. Phys. 24, 719 (1935).

27. G. B. Alexander, J. Phys. Chem. 61, 1563 (1957).

28. J. W. Christian, "Transformations in Metals and Alloys" Part I, Pergamon Press, 1974.

APPENDIX A

PREPARATION OF SUPERSATURATED SOLUTIONS

APPENDIX A

PREPARATION OF SUPERSATURATED SOLUTIONS

Supersaturated solutions of silicic acid were prepared at the desired temperature (generally 95°C) by mixing an alkaline solution of sodium silicate with a buffered brine to yield a final solution of the desired silicic acid concentration, pH, and salinity. In preliminary work, alkaline solutions of silica were prepared from sodium metasilicate. These solutions were not entirely satisfactory either in terms of purity or composition. According to Alexander (4), such solutions contain appreciable amounts of oligomer. Accordingly, sodium silicate solutions were prepared by dissolving, in doubly distilled water, a charge of spectroscopic grade SiO_2 (six nines purity) fused with reagent grade Na_2CO_3 (Mallinkrodt primary standard) in a molar ratio of SiO_2/Na_2CO_3 of 1:4. Fusion was carried out in a platinum crucible. According to Alexander (4), and from our results presented later, this procedure insures that silica is present as the monomer.

1. Preparation of Supersaturated Silica Solutions

Simulated brines supersaturated in silica were prepared by acidification of aliquots of the stock sodium silicate solution. The stock silica solution (containing about 1700 to 2000 ppm SiO_2) and the acidified brines were thermostated in an oil bath at temperatures in the range 75° to 105°C. After thermal equilibration, the stock solution was added to the brine as a thin stream under vigorous stirring. Transfer was accomplished by pressurizing the stock solution with N_2. The total transfer time was 10-30 sec; the temperature fluctuation during transfer was less than 2°C.

The acidified brine contained NaCl, KCl, and varying amounts of HCl, NaAc, and HAc (where Ac = acetate). Since the silicate solution is alkaline (pH $\sim$13), the composition of the brine must be adjusted to obtain at each silica concentration the desired final pH (in the range 4.5 to 6.5) and total salt concentration. The adjustment was made by a preliminary titration (at room temperature) of a brine containing the desired amount of silicate. With the help of such adjustments, we were able to control the final pH of the supersaturated silicic acid solution to within ± 0.05 pH unit.

Table A-1 gives two examples of solution preparation at two different silica concentrations at pH 4.5. The final concentrations of silica, Na^+, K^+, Cl^- and total acetate are given. These were essentially the same at a pH of 5.50, as can be seen from Table A-2.

Table A-1

A. Preparation of 1200 ppm (as SiO_2) Solution at pH = 4.50

The stock silicate solution was 0.0333M (2000 ppm as SiO_2) and contained Na^+ at a concentration of 0.2516M (molar ratio of Na^+ to SiO_2 of 8:1). The stock brine was prepared by mixing 25.00 cc of 1.020N HAc containing 0.325M KCl and 1.068M NaAc with 25.00 cc of a solution containing 0.435M NaCl and 0.815M HCl. After thermal equilibration at 95.0°C, 75.00 cc of the silicate solution was added as a thin stream to the brine with vigorous stirring. Final quantities of various species were as follows:

Na^+:	56.445	mmoles	in 125 cc or 0.452M or	10,400 ppm
K^+ :	8.130	"	in 125 cc or 0.065M or	2,540 ppm
Cl^-:	39.375	"	in 125 cc or 0.315M or	11,200 ppm
Ac^-:	25.200	"	in 125 cc or 0.202M or	11,900 ppm
HAc:	27.000	"	in 125 cc or 0.216M	

B. Preparation of 1000 ppm (as SiO_2) Solution at pH = 4.50

The stock silicate solution was 0.0278M (1667 ppm as SiO_2) and contained Na^+ at a concentration of 0.2094M. The stock brine was prepared by mixing 25.00 cc of 1.112N HAc containing 0.325M KCl and 1.068M NaAc with 25.00 cc of a solution containing 0.566M NaCl and 0.684M HCl. After thermal equilibration at 95.0°C, 75.00 cc of the silicate solution was added as a thin stream to the brine with vigorous stirring. Final quantities of various species were as follows:

Na^+:	56.555	mmoles	in 125 cc or 0.452M or	10,400 ppm
K^+ :	8.130	"	in 125 cc or 0.065M or	2,540 ppm
Cl^-:	39.375	"	in 125 cc or 0.315M or	11,200 ppm
Ac^-:	25.310	"	in 125 cc or 0.202M or	11,900 ppm
HAc:	29.250	"	in 125 cc or 0·234M	

Note: The apparent pK for HAc in brines with the above salt content is 4.5 as derived from data at pH = 4.50 and 4.4 as derived from data at pH = 5.50. The pK of HAc in aqueous solution (zero ionic strength) is 4.75.

Table A-2

Solution Compositions

A. pH = 4.50

Silicic Acid (as ppm SiO_2)	900	1000	1100	1200
Na^+, molar and (ppm)	0.448M (10,300)	0.452M (10,400)	0.452M (10,400)	0.452M (10,400)
K^+, molar and (ppm)	0.065M (2,540)	0.065M (2,540)	0.065M (2,540)	0.065M (2,540)
Cl^-, molar and (ppm)	0.315M (11,200)	0.315M (11,200)	0.315M (11,200)	0.315M (11,200)
Ac^-, molar and (ppm)	0.198M (11,600)	0.202M (11,900)	0.202M (11,900)	0.202M (11,900)
HAc, molar	0.228M	0.234M	0.205M	0.216M

B. pH = 5.50

Silicic Acid (as ppm SiO_2)	740	800	900	1000	1100
Na^+, molar and (ppm)	0.452M (10,400)	0.450M (10,400)	0.448M (10,300)	0.452M (10,400)	0.452M (10,400)
K^+, molar and (ppm)	0.065M (2,540)	0.065M (2,540)	0.065M (2,540)	0.065M (2,540)	0.065M (2,540)
Cl^-, molar and (ppm)	0.315M (11,200)	0.315M (11,200)	0.315M (11,200)	0.315M (11,200)	0.315M (11,200)
Ac^-, molar and (ppm)	0.202M (11,900)	0.200M (11,800)	0.198M (11,600)	0.202M (11,900)	0.202M (11,900)
HAc, molar	0.012M	0.014M	0.016M	0.012M	0.012M

The buffering capacity of acetate is negligible at pH greater than 5.50. Accordingly, maleate was substituted for acetate; otherwise, the brine composition was not altered. Kinetic runs for silica condensation at a pH 5.50 using acetate and maleate buffers yielded essentially identical results.

The pH values given here were measured at room temperature (∿25°C). Over the temperature range investigated (75° to 105°C), the pH varies by less than 0.1 unit (see Figure A-1).

Reaction vessels and auxiliaries were of Teflon. Other containers were of polyethylene. Glass did not come into contact with any of the supersaturated silica solutions. Silica stock solutions were made up to volume in Pyrex volumetric flasks and stored in polyethylene containers.

2. Mixing Conditions During Solution Preparation

The preparation of supersaturated solutions according to the procedure described above allows for convenient control of concentration, temperature, pH, and salt content; however, this technique generally presents difficulties in ensuring that conditions during mixing do not lead to artifically high nucleation rates because of large local supersaturations and, in this case, high local pH during mixing. There are at least two tests that can be applied for assessing the extent and importance of nucleation during mixing: (a) effects of variations in mixing conditions and (b) initial kinetics of condensation, particularly the time dependence of the initial phases of the condensation process.

(a) Variations in Mixing Conditions. It is clear, from elementary considerations, that the alkaline solution of sodium silicate must be added to the buffered salt solution (rather than the reverse), if the pH variation during mixing is to be kept at a minimum. This expectation was confirmed by tests which showed that addition of the buffered brine to the sodium silicate solution resulted in significantly greater condensation rates.

Aside from this, the most direct test of effects arising during the mixing process is to vary the concentration of the stock silicate solution (and, hence, the relative volumes of the silicate and buffered brine to be mixed). Results of one such series of tests are shown in Figure A-2. Here, the stock solution concentration was varied from 2500 ppm (as SiO_2) to 1250 ppm and the volume of silicate to buffered brine from 50/75 to 100/25. In all cases, the final concentration of silicic acid was nominally 1000 ppm (as SiO_2) and the final pH was 4.70. It is clear, from the figure, that variations in kinetic results are relatively small and, to a first approximation, rates are independent of the stock solution concentration and mixing volumes. We may infer that nucleation during

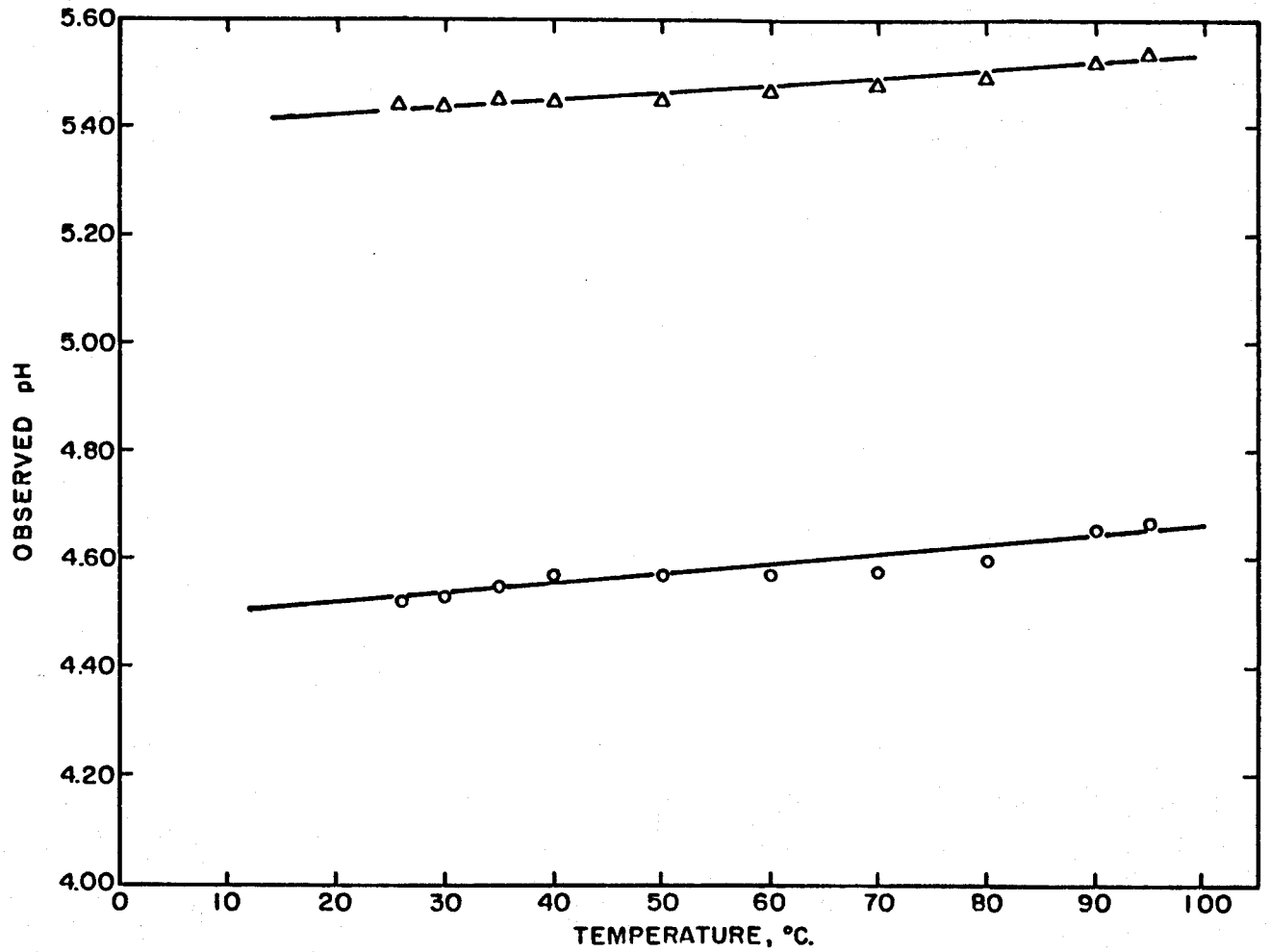

Fig. A-1: pH of silica-brine solutions as a function of temperature.

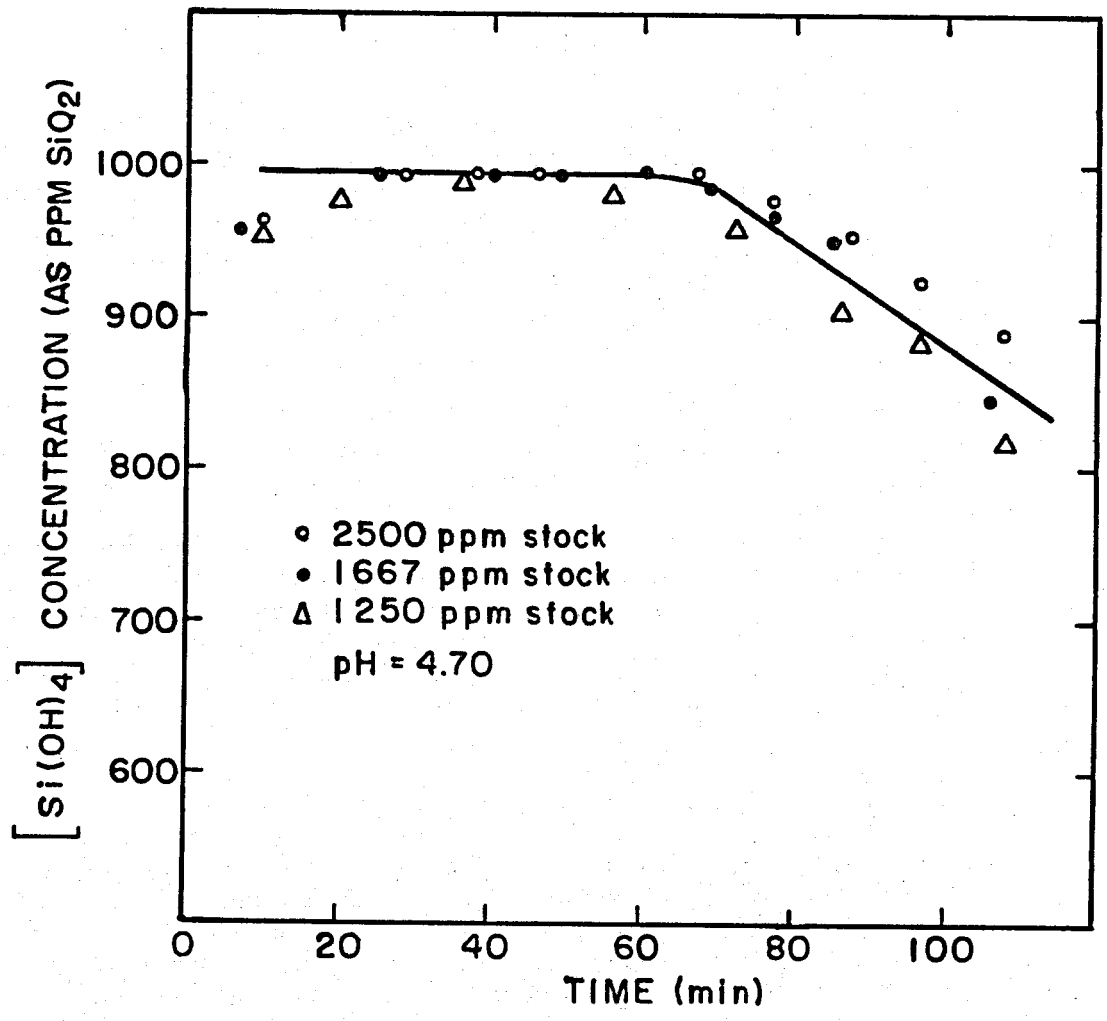

Fig. A-2: Silica condensation as a function of time from a 1000 ppm supersaturated solution prepared in different ways (see text).

mixing does not play a predominant role and that mixing conditions are not critical. This conclusion must be modified by the observation noted and discussed below.

(b) Initial Kinetics. In general, the expected kinetics of condensation in the initial stages are described by

$$x = 1-e^{-(t/\tau)^n}$$

where $x = (C_o-C_t)/(C_o-C_e)$, with C_o the initial concentration, C_t that at time t and C_e the (final) equilibrium concentration; t the time; τ a constant; and n an exponent expected to be between 3 and 4 (6). A value of 3 is expected when nucleation essentially occurs at an early stage in the reaction, that is, during mixing; a value of 4 is expected when the nucleation rate is constant throughout the reaction interval considered; an intermediate value describes cases where the nucleation rate is some decreasing function of time (7).

In our case, a plot of $\ln[-\ln(1-x)]$ vs. $\ln t$ would be expected to have a slope near 3 if nucleation was essentially complete during mixing; alternatively, a slope near 4 would correspond to a small (or negligible) contribution from nuclei formed during mixing. Relevant data are given in Table A-3 and corresponding plots are shown in Figure A-3 for various mixing conditions. Solid lines with a slope of 4 have been drawn; a dashed line with a slope of 3 is also shown. It is apparent that the data fit a relation with $n \sim 4$. We may conclude that nucleation during mixing is not the predominant mode of nuclei formation, that is, it makes a relatively small contribution to the overall number of nuclei eventually formed.

Besides the plot for a run at pH = 4.70, two other plots for pH = 4.50 are shown. In both cases at the latter pH, supersaturated solutions were prepared by using a stock solution 1667 ppm in silica as SiO_2. However, in one case the stock solution was added to the buffered brine; in the other, the stock solution was added to an acid solution of NaCl and HCl and the pH was then adjusted to its final value (of 4.50) by addition of a NaAc-HAc solution. The actual preparation involved adding 75 cc of the alkaline solution of silica of concentration 1667 ppm as SiO_2 to 25 cc of a solution 0.566M NaCl, 0.684M HCl and 0.0112M HAc, followed by addition to this mixture of 25 cc of a solution 0.325M in KCl, 1.068M in NaAc and 1.000N in HAc. As is apparent from Figure A-3, there is a small displacement on the time axis between the two cases. This suggests that in the second case some nuclei (or, more precisely, a larger number of nuclei) were formed during the mixing process. This is understandable since in the second case the supersaturated solution was

Table A-3

Run 1

2550 ppm stock to buffered brine to yield C_o = 985 ppm at pH = 4.70

t (min)	C_t (ppm SiO_2)	x	
76	968	0.0276	
87	942	0.0699	
96	915	0.114	C_e = 370 ppm
107	880	0.171	T = 95°C
118	845	0.228	
130	801	0.299	

Run 2

1667 ppm stock to buffered brine to yield C_o = 986 ppm at pH = 4.50

t (min)	C_t (ppm SiO_2)	x	
108	968	0.0276	
122	959	0.0423	
137	942	0.0699	
148	950	0.0569	C_e = 370 ppm
167	906	0.128	T = 95°C
180	880	0.171	
195	862	0.200	
210	835	0.244	

Run 3

1667 ppm stock to acid solution, then buffered to yield C_o = 985 ppm at pH = 4.50

t (min)	C_t (ppm SiO_2)	x	
110	950	0.0569	
119	959	0.0423	
128	932	0.0862	
137	924	0.0992	C_e = 370 ppm
146	899	0.140	T = 95°C
160	845	0.228	
174	818	0.272	

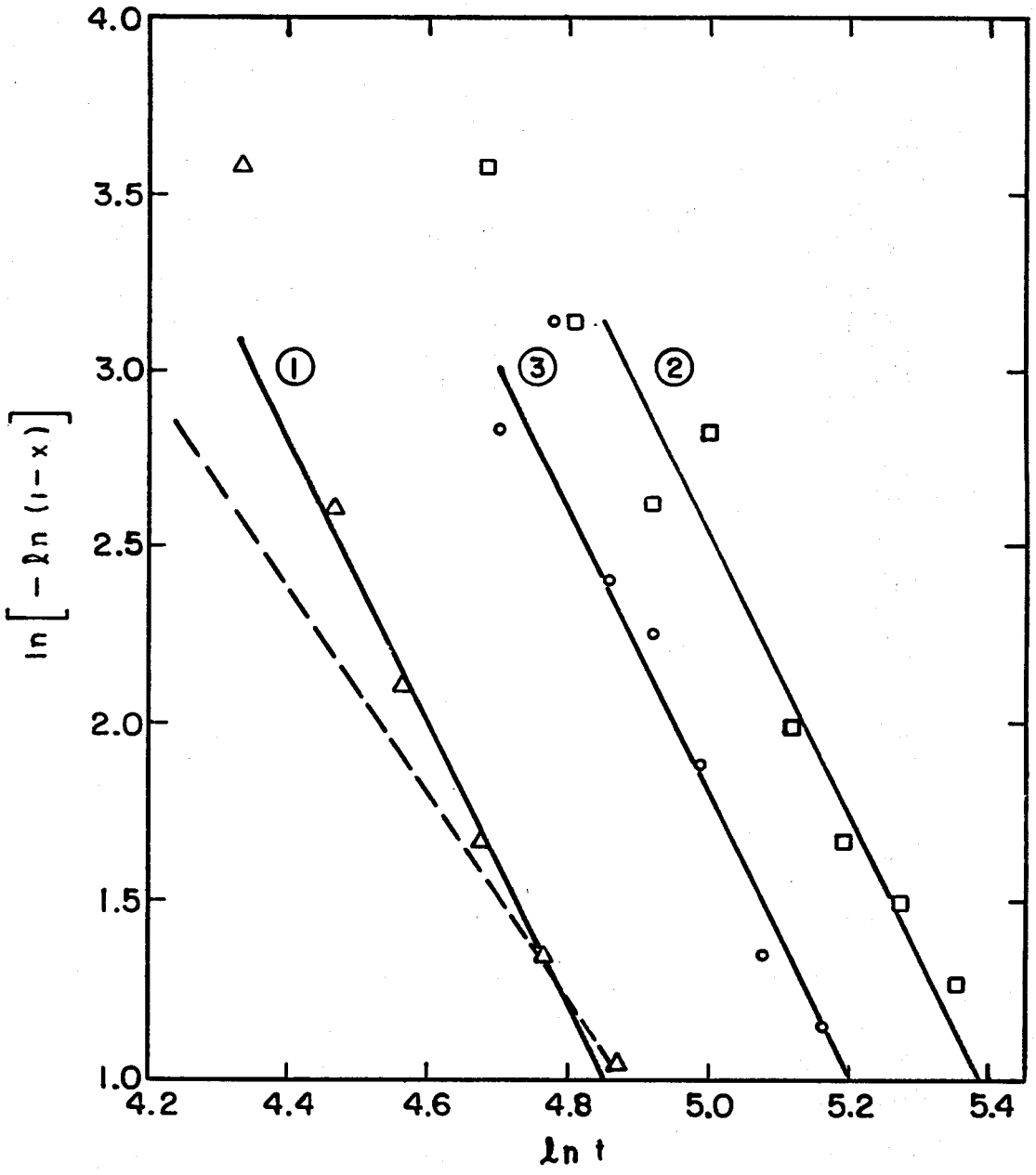

Fig. A-3: Kinetic plots of initial stages of condensation. Runs 1, 2 and 3 of Table A-3. Solid lines n = 4; dashed line n = 3.

for some time at a higher supersaturation and a low pH (∿0.3 to about 2), i.e., under conditions leading to a higher nucleation rate.

(c) Other Effects of Mixing. Generally, the amount of silicic acid in solution, as determined analytically with the molybdate method, was somewhat lower than expected (from the known volumes and concentrations) in the first few (10 to 20) minutes after mixing - although at longer times it increased to the expected value. The difference was usually about 2% (e.g., 20 ppm at 1000 ppm). The lower concentration cannot be a result of nucleation - not only because the amount of silica in nuclei is negligible, but also because nuclei will not redissolve, once formed, in a supersatured solution. Apparently, monomer silicic acid is removed by formation of non-equilibrium concentrations of species leading up to the critical size nucleus. These species do not readily react with molybdate (see Appendix B) and hence are not detected by the analytical technique. Such species include trimer, tetramer, pentamer, etc. All of these are unstable and will redissolve. Apparently, the equilibrium distribution of concentrations of various intermediates leading up to the critical size nucleus is re-established some time after mixing.

It is apparent, therefore, that during mixing, the high local concentration of silicate (silicic acid) and the high pH lead to a relatively high concentration of intermediate species. As the pH of each volume of added solution is lowered by mixing, some of these species are "frozen-in" since the kinetics are significantly slower at lower pH's (e.g., a factor of $\sim 10^4$ between pH 5 and 9). Some nuclei are probably also formed during mixing. Furthermore, for some time after mixing, nucleation is taking place from a solution with a "frozen-in" concentration of intermediates significantly higher than at the steady state.

To control these effects, variations in the mixing conditions were kept as small as possible. For example, the runs reported for final pH's of 4.50, 5.50 and "standard" brines (see Table A-2) were prepared by mixing volumes of stock solution with buffered brine according to the schedule given in Table A-4. Under these conditions, the observed transition times (see main text and Appendix C) can be interpreted with some confidence. The effects of mixing are not eliminated, but are held nearly constant.

We may note, finally, that the problems associated with mixing become more severe as the final pH of the mixed solution is raised. The problems presented by mixing are manageable when the final pH is in the range of 4.5 to 5.5. Some runs were carried out at a final pH of 6.50; the results are qualitatively consistent with those at pH of 4.5 to 5.5, but quantitative comparisons are obscured by effects of mixing.

Table A-4

pH = 4.50

Stock Solution (ppm SiO_2)	Volume Stock Solution	Volume Buffered Brine	Final Concentration (ppm SiO_2)
1667	67	58	900
1667	75	50	1000
1667	83	42	1100
2000	75	50	1200

pH = 5.50

1667	55	70	740
1667	60	65	800
1667	83	42	1100

APPENDIX B

ANALYSIS OF DISSOLVED SILICIC ACID

APPENDIX B

ANALYSIS OF DISSOLVED SILICIC ACID

The determination of silicic acid concentration was based on the β-complex of silicic acid with molybdate (3) and generally followed the method recommended by Alexander (4). The major modification was in the acidification step. In our procedure, acidification was carried out at a temperature of 25°C; the total concentration of silicic acid in the acidified solution was kept to less than 0.15 mg/ml as SiO_2. In the procedure described by Alexander, the acidification temperature was 2°C and the total concentration less than 1.0 mg/ml. As observed by others (5) and confirmed by us, the latter procedure leads to nonlinearity of absorbance with $Si(OH)_4$ concentration.

1. Procedure

An aliquot (usually 1.00 cc) of the solution to be analyzed was pipetted as a thin stream into a vigorously stirred solution of H_2SO_4. Volumes and concentrations were adjusted so as to yield an acidified solution with a final pH of 2.0 ± 0.5 and SiO_2 concentration less than 0.15 mg/ml. An aliquot (usually 100 µl) of the acidified sample was injected into freshly prepared, 0.4% ammonium molybdate tetrahydrate (FW 1235.86) in 0.1N H_2SO_4 obtained by mixing 4 cc of a stock 10% ammonium molybdate tetrahydrate solution in ∿60 cc H_2O, adding 10 cc of N H_2SO_4 and diluting to a total volume of 100 cc (4). The dilution ratio was 1:30 (100 µl of sample injected in 3 cc of molybdate solution). The molybdate solution was thermostated at 25.0 ± 0.2°C. Color development was followed at 400 nm as a function of time (readings at 7.5 sec intervals) until no further change was observed.

When analyzing aliquots from supersaturated solutions undergoing condensation, about 1.5 cc was withdrawn and quenched in an ice bath for 90 sec. After this time, the temperature of the sample was ca. 35°C and its density was negligibly (for analytical purposes) different from the density at 25°C. A measured quantity (1.00 cc) was withdrawn, acidified, and analyzed as described above. If the solution had an appreciable amount of colloidal silica, a blank from the acidified solution was also run and the results corrected for scattering by colloidal silica. Even in late stages of the condensation reaction, corrections for scattering did not exceed about 5% of observed absorbances.

Using the analytical procedure described above, a linear relation is observed between absorbance and $Si(OH)_4$ concentration over the range

of concentrations used in this work (see Figure B-1). The optical density of a solution containing 2.00 mg of SiO_2 per 100 ml of color developing solution is 0.748 which is to be compared with 0.720 reported by Alexander (4).

We may note that the complex formed (and corresponding absorbance) is sensitive to the pH of the color-forming solution (see ref. 8 and also Figure B-2 reproduced from ref. 3). The pH of the color forming solution used here was 1.30.

The rate of color development depends on pH, temperature, and H^+/ molybdate ratio (8). If the kinetics of color development are of interest, it is essential that the solution be thermostated during the spectrophotometric measurements. Under conditions employed here (solution 2.27×10^{-3}M in Mo, pH = 1.3, ratio of acid to molybdate = 4.40), β-molybdosilicic acid is formed according to a reaction obeying first order kinetics with a rate constant $k_1' = 2.1$ min^{-1} at 25.0°C (see Figure B-3). The value of k_1' reported by Alexander (4) under somewhat different conditions was 2.3 min^{-1} (room temperature).

The dependence of the first order rate constant on temperature (see Figure B-4) yields an activation energy under conditions employed here (pH = 1.30, molybdate concentration 0.011M) of 14.35 kcal/mol.

2. Analysis for Dimer of Silicic Acid

Alexander (4) showed that with progressively increasing molecular weight of the silicic acid species in solution, the reaction rate with molybdate decreases. For the dimer, Alexander suggested that it reacted by consecutive first order reactions (dimer → monomer → β-complex) but yet treated the overall reaction as apparently first order with a rate constant of $k_2' = 0.9$ min^{-1}.

Under comparable conditions to the ones employed here (pH = 1.4, 4 g/l of molybdate, 25°C, concentration of silica of the order of 2.5 mg/ml), Couduner, Baudru and Donnet (9) found k_1' (monomer) = 2.1 min^{-1} and $k_2' = 0.9$ min^{-1}. These authors suggest that dimer reacts directly with molybdate, although the arguments advanced for this suggestion are indirect. Interpretation of their results is somewhat complicated by the presence of higher oligomers reacting with an apparent rate constant $\sim$0.18 min^{-1}.

Other authors (10-12) present results for various conditions showing first order reactions for dimer and higher oligomers. The values of the rate constants vary with conditions, but are always in the order $k_1' > k_2' >> k_3' >> k_n'$ for higher oligomers.

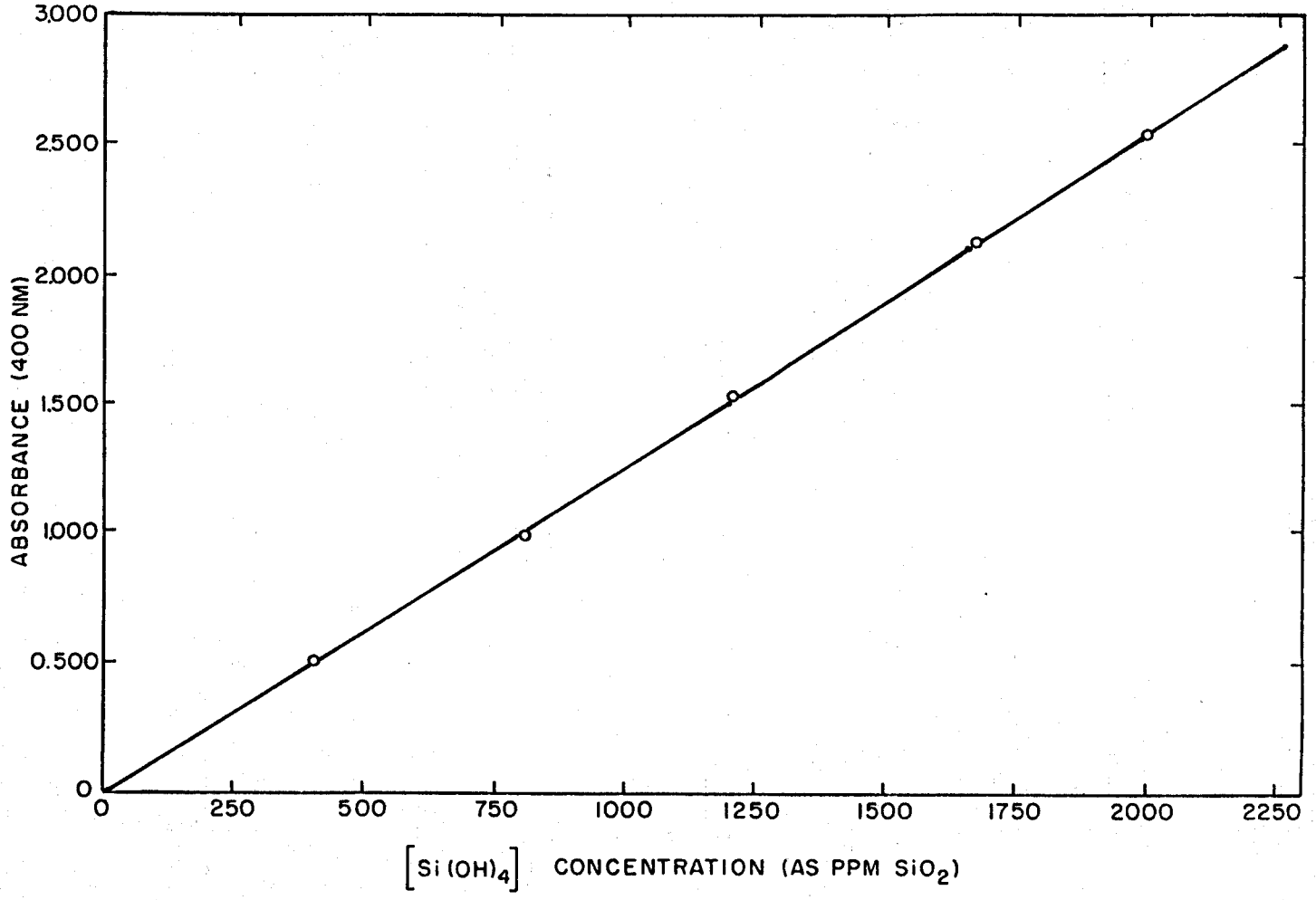

Fig. B-1: Calibration curve for a series of stock silica solutions. Each point represents a solution prepared from a separate fusion of SiO_2 with Na_2CO_3. Absorbances are for 100 µl injected in 3 cc of molybdate solution (after suitable correction for dilution during acidification).

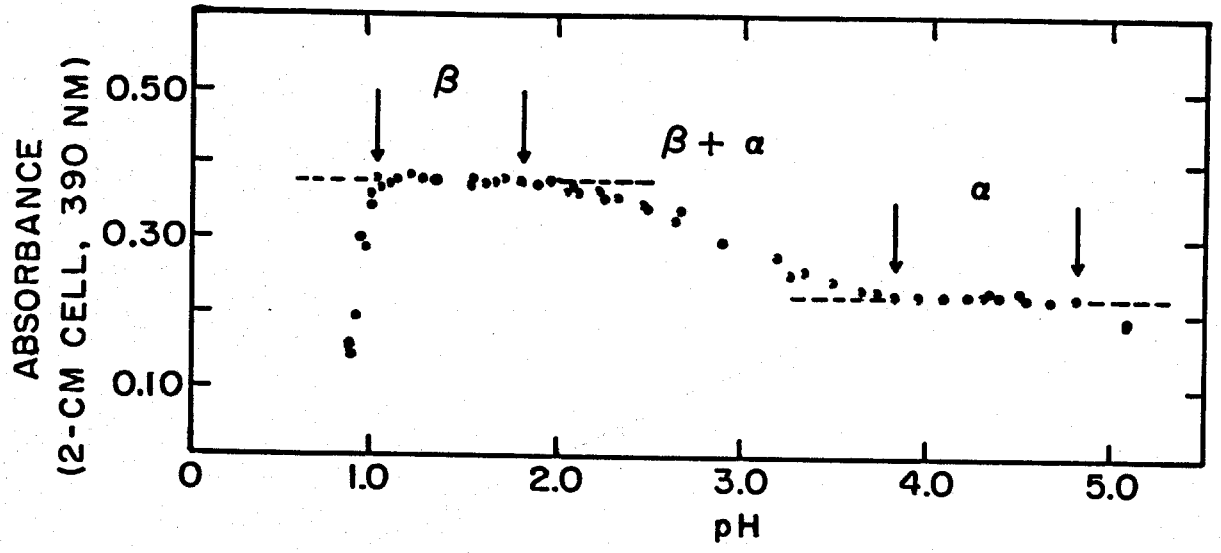

Fig. B-2: pH stability ranges for formation of α and β molybdosilicate complexes (see ref. 3).

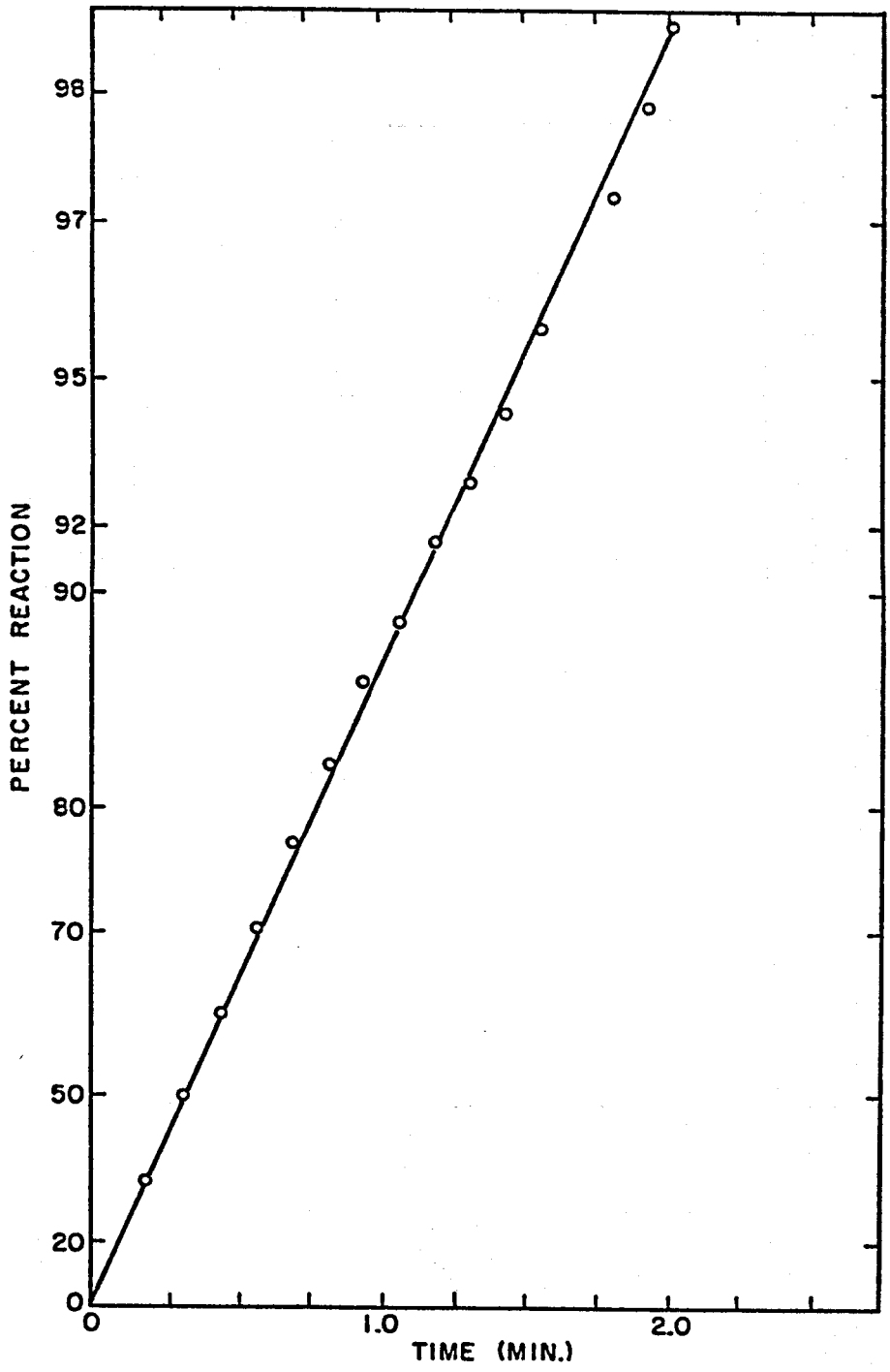

Fig. B-3: First order kinetic plot for color development for $Si(OH)_4$ in molybdate solution (pH = 1.3) at 25°C.

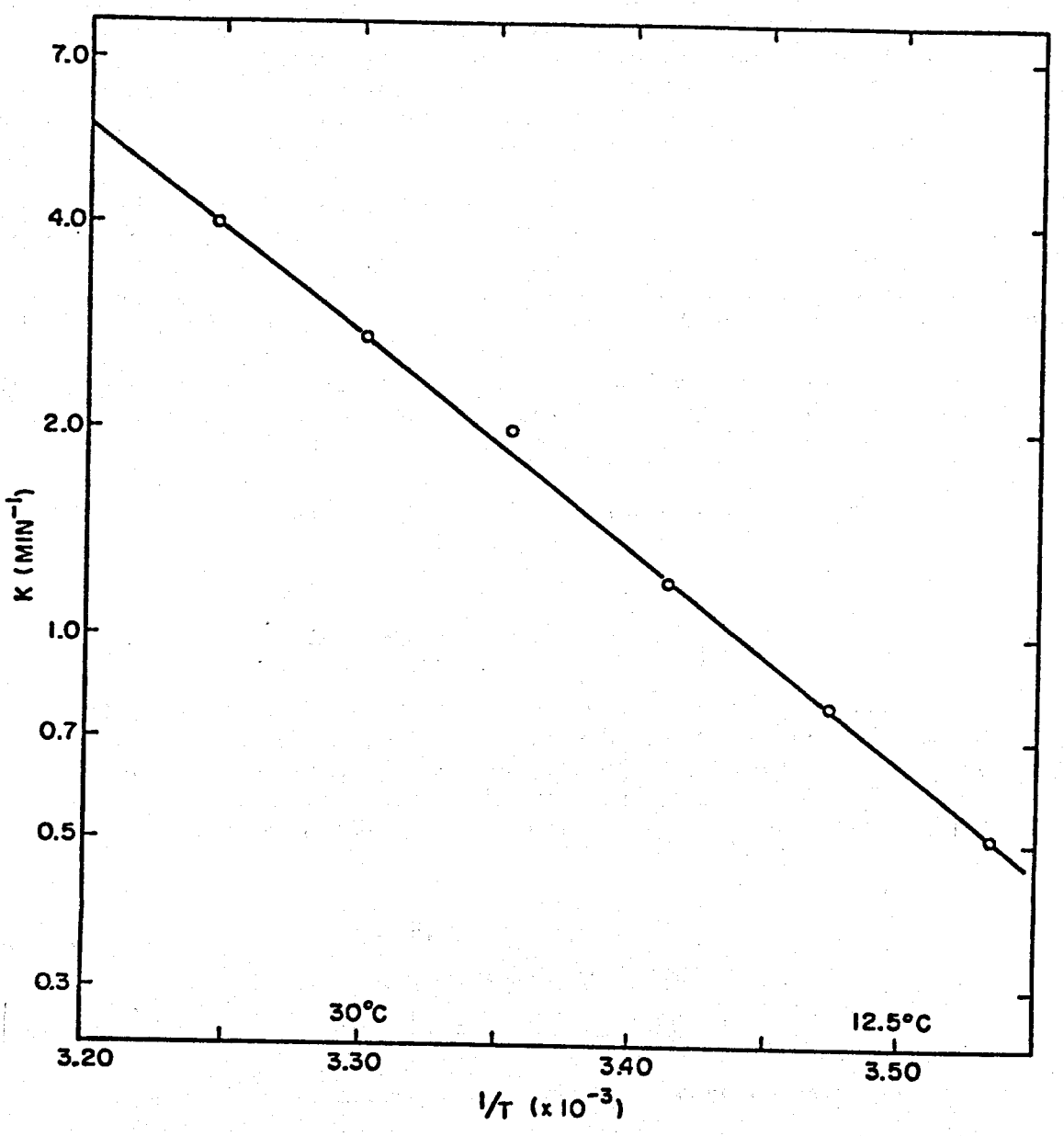

Fig. B-4: The rate constant for color development by $Si(OH)_4$ in molybdate solutions (pH = 1.30) as a function of temperature.

To establish appropriate values for conditions used here, we prepared more or less pure dimer by hydrolysis of hexachlorosilane. Hydrolysis is sufficiently rapid compared to subsequent reaction (either decomposition to the monomer or condensation to higher species) to yield essentially only dimer. Dimer solutions were prepared by injecting 300 µl of Si_2OCl_6 in 115 cc of distilled water held at 2°C (concentration of disilicic acid was 1667 ppm as SiO_2).

Using these solutions and the same molybdate solutions and procedure as for the monomer (except that dilution of the sample by injection into dilute H_2SO_4 was carried out at 2°C), kinetic data for the molybdate reaction were obtained at 25°C and shown in Figure B-5. It is apparent that first order reaction kinetics are obeyed with $k_2' = 0.82\ min^{-1}$.

This result allows us to make certain deductions about the mechanism of formation of the β-complex. Clearly, dimer reacts directly with molybdate, i.e., the reaction follows the path

$$\text{dimer} + \text{molybdate} \rightarrow \beta\text{-complex}$$

rather than

$$\text{dimer} \rightarrow \text{monomer} \rightarrow \beta\text{-complex}$$

However, the complex formed is the same, whether the starting material is the monomer or the dimer. The actual structure of the silicomolybdic complex is not known, but the Si:Mo ratio is always found to be 1:12. The complex may be pictured (10) as containing a silicon-oxygen tetrahedron at the center with four Mo_3O_9H groups attached to the oxygens:

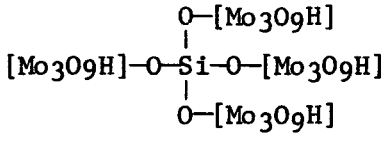

and is probably formed by a reaction with a sequence

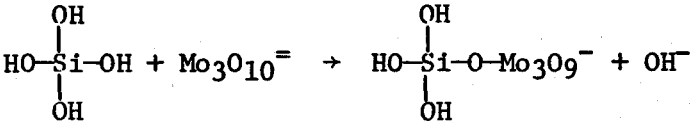

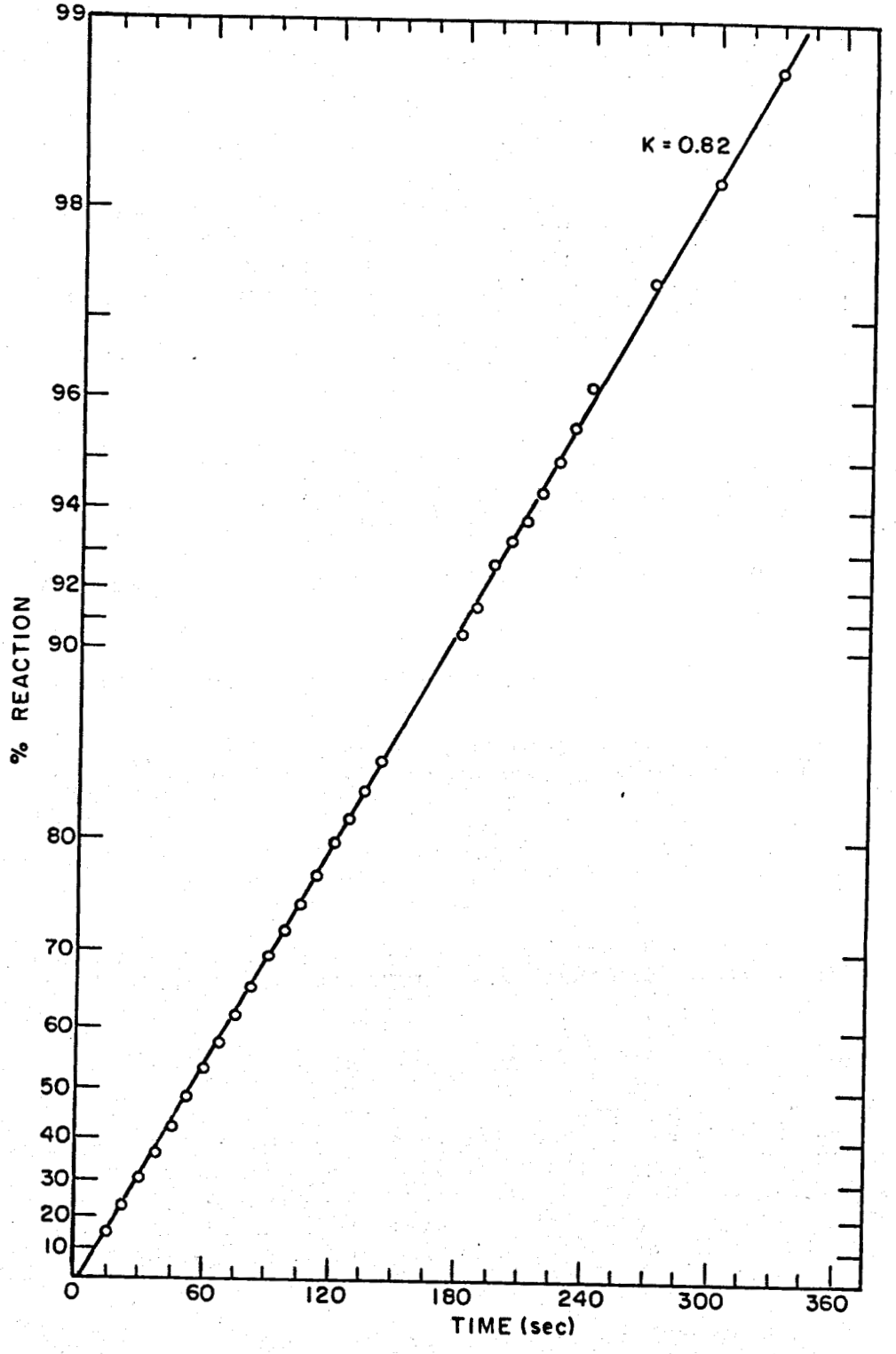

Fig. B-5: First order kinetic plot for color development for dimer of silicic acid in molybdate solution at 25°C.

In the sequence of reactions

$$Si(OH)_4 + B^- \rightarrow Si(OH)_3B \rightarrow Si(OH)_2B_2 \rightarrow Si(OH)B_3 \rightarrow SiB_4$$

where B^- is the molybdate group ($Mo_3O_{10}H$), the slow step corresponding to the rate constant k_1' is either the first or the last. In other words, substitution of B for OH either promotes further reaction or retards it. Although there is no direct evidence on this point, we think it likely that the first substitution is the slow step:

$$Si(OH)_4 + B^- \rightarrow Si(OH)_3B + OH^-$$

Subsequent reactions may be faster because of stabilization of the activated complexes, formed in the subsequent steps, by resonance contributions among the molybdate groups or for other reasons.

Corresponding reactions for dimer may involve a sequence beginning with

$$(HO)_3Si{-}O{-}Si(OH)_3 + Mo_3O_{10}H^- \rightarrow (HO)_2(Mo_3O_{10}H)Si{-}O{-}Si(OH)_3 + OH^-$$

and subsequent reactions yielding intermediates of a similar type. Further reaction between partially substituted dimer and $Mo_3O_{10}^-$ must then follow the path

$$B_3{-}Si{-}O{-}Si(OH)_3 + B^- \rightarrow B_3{-}Si{-}O^- + Si(OH)_3B$$

and must proceed at a higher rate than the original displacement of one of the hydroxyl groups. Alternatively, the initial step may be

$$(HO)_3{-}Si{-}O{-}Si(OH)_3 + Mo_3O_{10}^= \rightarrow -\overset{|}{\underset{|}{Si}}{-}O{-}Mo_3O_9^- + -\overset{|}{\underset{|}{Si}}{-}O^-$$

as has been suggested (5). In this case, $Si(OH)_3(OMo_3O_9H)$ would rapidly yield $Si(OM_3O_9H)_4$; however, the $Si(OH)_4$ produced in the rate-controlling step would exhibit a reaction rate identical to that of the monomer. This second mechanism is a combination between direct and sequential reactions, i.e., direct reaction of the dimer yields, in part, monomer which then also reacts to yield the complex.

The results presented above favor the sequence of reactions initiated by replacement of an -OH group on the dimer rather than attack at the

siloxane bond. The main evidence favoring this alternative is the absence of any indication of sequential reactions in the kinetic data for color development for the dimer. This is given considerable weight, since the rate constants ($k_1' = 2.1\ min^{-1}$ and $k_2' = 0.8\ min^{-1}$) are comparable.

APPENDIX C

INITIAL KINETICS OF NUCLEATION AND GROWTH OF SILICA

APPENDIX C

INITIAL KINETICS OF NUCLEATION AND GROWTH OF SILICA

We consider here the kinetics of nucleation and growth during initial stages of precipitation. We treat first the case of growth for a fixed number of nuclei and then consider nucleation as well as growth.

1. Interface Controlled Growth with a Fixed Number of Nuclei

Let C_o, C_t and C_e be the concentrations of solute initially, at time t, and at equilibrium, and denote by r_t the radius of a particle at time t. Then

$$C_o - C_t = \frac{n}{V^S} \frac{4\pi}{3} r_t^3 \qquad \text{(C-1)}$$

where n is the number of particles (assumed fixed) per unit volume and V^S is the molar volume of the precipitate ($V^S = Nv_S$ with N = Avogadro's number). From Eq. (C-1) we obtain

$$-\frac{dC_t}{dt} = -\dot{C}_t = \frac{4\pi n}{V^S} r_t^2 \dot{r}_t \qquad \text{(C-2)}$$

The rate of growth, if interface controlled, is also given by

$$-\dot{C}_t = k_1 C_t A_t - k_2 A_t \qquad \text{(C-3)}$$

where A_t is the area of the precipitate per unit volume at time t and k_1 is the reaction rate constant (cm/sec). From the condition of equilibrium,

$$k_2 = k_1 C_e \qquad \text{(C-4)}$$

Therefore,

$$-\dot{C}_t = k_1 A_t (C_t - C_e) \qquad \text{(C-5)}$$

Accordingly, from Eq. (C-2) and Eq. (C-5)

$$\dot{r}_t = k_1 V^S (C_t - C_e) = \mathring{k}_1 \lambda V^S (C_t - C_e) \qquad \text{(C-6)}$$

with k_1(cm/sec) = $\overset{\circ}{k_1}$(sec^{-1}) λ (molecular diameter, cm). Substituting Eq. (C-1) and Eq. (C-6) into Eq. (C-2) we obtain:

$$-\dot{C}_t = \left[36\ \pi n(V^S)^2\right]^{1/3}\ \overset{\circ}{k_1}\lambda\left(C_o-C_t\right)^{2/3}\left(C_t-C_e\right) \qquad \text{(C-7)}$$

If we define

$$x = \frac{C_o-C_t}{C_o-C_e} \text{ and } \dot{x} = -\frac{\dot{C}_t}{C_o-C_e} \qquad \text{(C-8a,b)}$$

we can rewrite Eq. (C-7) as

$$\dot{x} = \left[36\ \pi n(V^S)^2\right]^{1/3}\ \overset{\circ}{k_1}\lambda\left(C_o-C_e\right)^{2/3}\ x^{2/3}\left(1-x\right) \qquad \text{(C-9)}$$

or, alternatively,

$$\frac{dx}{x^{2/3}(1-x)} = \alpha dt \qquad \text{(C-10)}$$

where

$$\alpha = \left[36\ \pi n(V^S)^2\ (C_o-C_e)^2\right]^{1/3}\overset{\circ}{k_1}\lambda \qquad \text{(C-11)}$$

The differential equation (C-10) can be simplified when x is small (i.e., when C_o-C_t is small) by approximating 1-x by 1. With this approximation

$$\frac{dx}{x^{2/3}(1-x)} \simeq \frac{dx}{x^{2/3}} \simeq \alpha dt \qquad \text{(C-12)}$$

Therefore,

$$x^{2/3} \simeq \frac{\alpha^2 t^2}{9} \qquad \text{(C-13)}$$

Substituting (C-13) into (C-12) we obtain

$$\frac{dx}{1-x} \simeq \frac{\alpha^3}{9}\ t^2 dt \qquad \text{(C-14)}$$

which yields upon integration

$$x \simeq 1-\exp\left[-\left(\frac{\alpha}{3}\right)^3 t^3\right] \qquad \text{(C-15)}$$

or
$$\frac{C_o-C_t}{C_o-C_e} = 1-\exp\left[-\left(\frac{\alpha}{3}\right)^3 t^3\right] \qquad \text{(C-16)}$$

Equation (C-16) is expected to apply for growth of a fixed number of nuclei (presumably formed during the mixing process), provided the reaction kinetics are controlled by the reaction step at the interface. Under these conditions, and for small values of x, a plot of $\ln[-\ln(1-x)]$ against $\ln t$ should be linear with a slope of 3.

2. Nucleation and Growth

If the number of nuclei is not fixed at the beginning of the precipitation process but nucleation is occurring during the course of the reaction, the situation is more complex. Let it be assumed that between times $t = \tau$ and $\tau + \delta\tau$, a number of new nuclei are formed. The volume of particles nucleated at time $t = \tau$ is

$$V_\tau = \frac{4\pi}{3} Y^3(t-\tau)^3 \text{ for } t>\tau \qquad \text{(C-17)}$$

$$V_\tau = 0 \text{ for } t\leq\tau \qquad \text{(C-18)}$$

where Y is the rate of growth of nucleated particles. The volume of precipitate per unit volume of solution at time $\underline{t}$ is then given by

$$V_\tau = \frac{4\pi}{3}\int_{\tau=0}^{t} I\, Y^3(t-\tau)^3 d\tau \qquad \text{(C-19)}$$

where I is the nucleation rate per unit volume. The equation can be integrated by making some assumptions about the dependence of I on time. Within similar approximation as made before for a fixed number of nuclei, we may take Y and I in Eq. (C-19) as fixed so that

$$V_\tau = \frac{\pi}{3} I\, Y^3 t^4 = \frac{\pi}{3}(It)Y^3 t^3 \qquad \text{(C-20)}$$

This equation is analogous to Eq. (C-1) with $\underline{n}$ replaced by It and $\bar{r}_t = Yt$, where $\bar{r}_t$ is the average radius of particles at time t. Accordingly,

$$C_o-C_t = \frac{It}{V^S}\frac{\pi}{3}\bar{r}_t^3 \qquad \text{(C-21)}$$

and

$$-\dot{C}_t = \frac{I}{V^S}\frac{\pi}{3}\bar{r}_t^3 + \frac{It}{V^S}\pi(\bar{r}_t)^2\,\dot{\bar{r}}_t \qquad \text{(C-22)}$$

If the rate of growth is interface controlled, we have, as before, by using the same substitutions and with $x = C_o - C_t / C_o - C_e$,

$$\dot{x} = \left[\frac{64\pi}{3} I(V^S)^2 (C_o - C_e)^2\right]^{1/3} k_1 \, t^{1/3} \, x^{2/3} (1-x) \qquad \text{(C-23)}$$

$$\frac{dx}{x^{2/3}(1-x)} = \alpha' t^{1/3} dt \qquad \text{(C-24)}$$

with

$$\alpha' = \left[\frac{64\pi}{3} I(V^S)^2 (C_o - C_e)^2\right]^{1/3} k_1^{\circ} \lambda \qquad \text{(C-25)}$$

Making the same approximations as before we obtain

$$\frac{C_o - C_t}{C_o - C_e} = 1 - \exp\left[-\left(\frac{\alpha'}{4}\right)^3 t^4\right] \qquad \text{(C-26)}$$

3. The Transition Period

The kinetic runs show an initial period, whose extend depends on C_o, during which there is no detectable change in dissolved silicic acid. In effect, the rate of removal of material from solution during this time is below the detection limit of the analytical technique. Let us assume that the detection limit of concentration change is ΔC (say, 10 ppm, independent of C_o). The transition time, τ', is then

$$\Delta C = -\int_0^{\tau'} \dot{C}_t dt \qquad \text{(C-27)}$$

(a) Transition Times for Fixed Number of Particles. If the number of nuclei is fixed (e.g., nucleation takes place during mixing and effectively ceases thereafter), then from Eq. (C-16), expanded around $x = 0$, we have

$$\frac{\Delta C}{C_o - C_e} = \frac{4\pi}{3}\left(k_1^{\circ}\lambda\right)^3 \left(C_o - C_e\right)^2 \left(V^S\right)^2 \, n\left(\tau'\right)^3 \qquad \text{(C-28)}$$

Accordingly, a plot of $\ln \tau'$ against $\ln[1/(C_o - C_e)]$ should be linear with a slope of about 1. If nuclei are formed during the mixing process, there may be a further dependence on C_o, yielding a slope somewhat greater than 1, perhaps as high as 2.

(b) Transition Times with Continuous Nucleation. If nucleation does not occur predominantly during mixing - or if nucleation during the apparent transition stage of the precipitation reaction contributes the predominant number of nuclei - then the transition time will be given by Eq. (C-26):

$$x = \frac{C_o - C_\tau'}{C_o - C_e} = \frac{\Delta C}{C_o - C_e} = \frac{\pi}{3}\left(k_1^\circ \lambda\right)^3 \left(C_o - C_e\right)^2 \left(v^S\right)^2 I \left(\tau'\right)^4 \qquad \text{(C-29)}$$

The relation between τ' and C_o includes the dependence of I on C_o. As noted in the text, this dependence is

$$I = (\text{Const}) \exp\left(- \frac{\beta}{(\ln C_o/C_e)^2}\right) \qquad \text{(C-30)}$$

Accordingly,

$$\ln \tau' = - \frac{3}{4} \ln (C_o - C_e) + \frac{\beta/4}{(\ln C_o/C_e)^2} + \text{Const.} \qquad \text{(C-31)}$$

Over a limited range of C_o, the second term in Eq. (C-31) will predominate and $\ln \tau'$ will vary primarily as $1/(\ln C_o/C_e)^2$. A plot of $\ln(\ln \tau')$ vs. $\ln[1/\ln(C_o/C_e)^2]$ should be linear with a slope of 1 or a plot of $\ln \tau'$ vs. $1/[\ln(C_o/C_e)^2]$ should be linear with a slope of $\beta/4$, as long as the variation in the term $\ln(C_o - C_e)$ can be neglected.

(c) Analysis of Observed Transition Time. Observed transition times and corresponding C_o/C_e values are given in Table C-1 and plotted in Figure C-1. The data conform to Eq. (C-31). The slope of a plot of $\ln(\tau')$ vs. $1/[\ln(C_o/C_e)]^2$ is approximately 6. According to Eq. (C-31), we have

$$\beta \cong 24 \cong \frac{\Delta G_c}{kT} \qquad \text{(C-32)}$$

where ΔG_c, defined in the main text, is the free energy of activation for nucleation. ΔG_c is given by (see main text)

$$\Delta G_c = \frac{16\pi v_S^2 \gamma_{SL}^3}{3(kT)^2} \qquad \text{(C-33)}$$

where v_S the molecular volume of SiO_2 and γ_{SL} the interfacial free energy between SiO_2 and the solution. With $v_S = 4.5 \times 10^{-23}$ cm^3/molecule,

$$\gamma^3 = 9.387 \times 10^{-17}$$

or

$$\gamma = 45 \text{ ergs/cm}^2$$

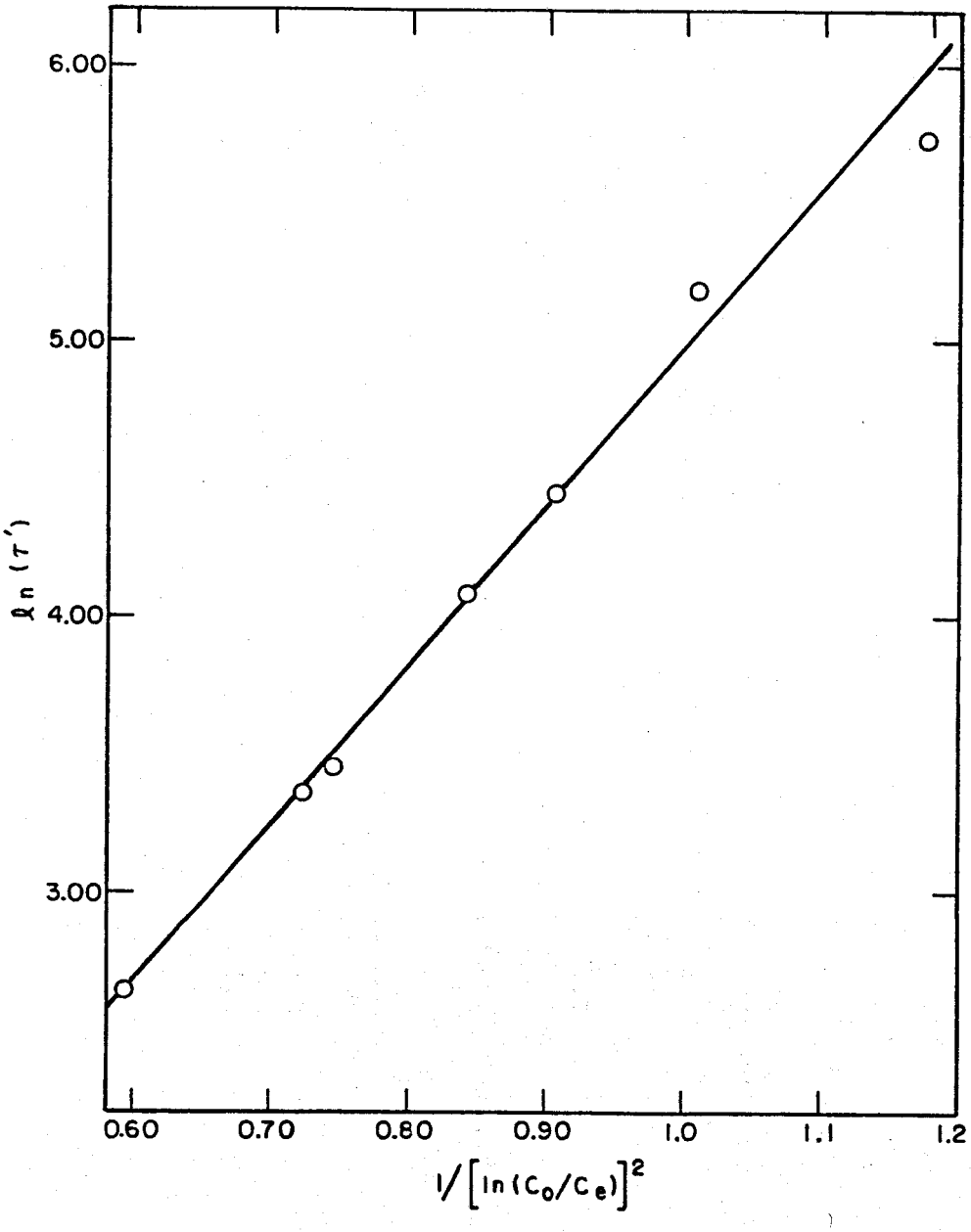

Fig. C-1: Transition times as a function of supersaturation.

Table C-1

Transition Times for Precipitation of Silica
(pH = 4.50 and T = 95.0°C)

A. Standard Brine

C_o (ppm as SiO_2)	C_e (ppm as SiO_2)	C_o/C_e	$1/[\ln(C_o/C_e)]^2$	τ' (min)	$\ln(\tau')$
1200	370	3.243	0.722	29	3.367
1100	370	2.973	0.842	60	4.094
1000	370	2.703	1.011	178	5.182
900	370	2.432	1.266	310	5.736

B. Various Brines with C_o = 1100 ppm

Chloride in Brine (M)	C_e (ppm as SiO_2)	C_o/C_e	$1/[\ln(C_o/C_e)]^2$	τ' (min)	$\ln(\tau')$
0.152	385	2.857	0.907	86	4.454
0.315	370	2.973	0.842	60	4.094
0.844	345	3.188	0.744	32	3.466
1.555	300	3.667	0.592	14	2.639

As shown in the main text, this value is consistent with reported values for the interfacial free energy and with results from the activation energy obtained from measurements at a series of temperatures between 75° and 105°C.

APPENDIX D

TEMPERATURE COEFFICIENT OF REACTION RATE

APPENDIX D

TEMPERATURE COEFFICIENT OF REACTION RATE

The Energy of Activation

The rate expression describing the kinetics in the initial stages of condensation is

$$\frac{C_o-C_t}{C_o-C_e} = 1 - \exp\left[\frac{\pi}{3}\left(v^S\right)^2\left(C_o-C_e\right)^2\left(k_1^\circ\lambda\right)^3 I t^4\right] \qquad (D\text{-}1)$$

The corresponding expression for the transition time, τ', is

$$\frac{\Delta C}{C_o-C_e} = \frac{\pi}{3}\left(k_1^\circ\lambda\right)^3\left(C_o-C_e\right)^2\left(v^S\right)^2\ I\left(\tau'\right)^4 \qquad (D\text{-}2)$$

Inspection of results for the temperature coefficient at pH = 4.50 and $\ln(C_o/C_e)$(at 95°C) ≃ 1 shows that condensation rates are only slightly changed by varying the temperature between 75° and 105°C. A similar near independence of overall condensation rates on temperature is also observed at pH = 5.50 and $\ln(C_o/C_e)$(at 95°C) ≃ 0.89. Therefore, we will assume that, to a first approximation, condensation rates are independent of temperature.

If we neglect the variation with temperature of pre-exponential terms, we may write the temperature coefficient as

$$\frac{d[\Delta C/(C_o-C_e)]}{d(1/T)} = 0 = \frac{d}{d(1/T)}\left[\left(k^\circ\right)^3 \cdot I\right] \qquad (D\text{-}3)$$

At any given pH, we may write

$$k_1^\circ = k_o \exp\left(-\frac{\Delta_\alpha g^\dagger}{kT}\right) \qquad (D\text{-}4)$$

where $\Delta_\alpha g^\dagger$, the activation free energy, was defined previously. Also

$$I = (\text{Constant}) \exp\left(\frac{-\Delta G_c-\Delta_\alpha g^\dagger}{kT}\right) \qquad (D\text{-}5)$$

where ΔG_c is the free energy of a nucleus of critical size.

From (D-3), (D-4) and (D-5), we have

$$\frac{d}{d(1/T)}\left[\left(k_1^\circ\right)^3 I\right] = \frac{d}{d(1/T)}\left(\frac{-\Delta G_c - 4\Delta_\alpha g^\dagger}{kT}\right) = 0 \qquad \text{(D-6)}$$

or

$$-\frac{\Delta G_c - 4\Delta_\alpha g^\dagger}{k} - \frac{1}{kT}\frac{d(\Delta G_c)}{d(1/T)} = 0 \qquad \text{(D-7)}$$

ΔG_c is given by

$$\Delta G_c = \frac{A}{k^2T^2[\ln(C_o/C_e)]^2} \qquad \text{(D-8)}$$

where A is a constant (see main text) essentially independent of temperature. Accordingly,

$$\frac{d(\Delta G_c)}{d(1/T)} = \frac{2A}{k^2T}\left[\ln(C_o/C_e)\right]^{-2} - \frac{2A}{k^2T^2}\left[\ln(C_o/C_e)\right]^{-1}\frac{d\ln C_e}{d(1/T)} \qquad \text{(D-9)}$$

Substituting in Eq. (D-7) and noting that

$$\frac{d\ln C_e}{d(1/T)} = \frac{\Delta H_{sln}}{k} \qquad \text{(D-10)}$$

where ΔH_{sln} is the heat of solution of SiO_2, we have

$$\Delta G_c + 4\Delta_\alpha g^\dagger = -2\Delta G_c + 2\Delta G_c\left(\frac{\Delta H_{sln}}{kT}\right)\left[\ln(C_o/C_e)\right] \qquad \text{(D-11)}$$

ΔH_{sln} is 2.65×10^3 cal/mol, or 4.40×10^{-21} cal/molecule. At 368°K,

$$\frac{\Delta H_{sln}}{kT} = 3.60$$

and $\ln(C_o/C_e) = \ln(1100/370) \simeq 1$. Accordingly,

$$4\Delta_\alpha g^\dagger = -3\Delta G_c + 7.2\ \Delta G_c \qquad \text{(D-12)}$$

As noted in the main text,

$$\Delta G_c = \frac{4}{3}\pi(r_c)^2\gamma_{SL} = \frac{16\pi v_S^2\gamma_{SL}^3}{3(kT)^2} \qquad \text{(D-13)}$$

where r_c is the radius of the nucleus of critical size, γ_{SL} the interfacial energy between SiO_2 and the solution, and v_S the molecular volume of SiO_2. Using

$$v_S = 4.5 \times 10^{-23} \text{ cm}^3/\text{molecule}$$

$$\gamma_{SL} = 45 \text{ ergs/cm}^2$$

$$kT = 5.1 \times 10^{-21} \text{ joule/molecule}$$

we have

$$\Delta G_c = \frac{(16)(3.14)(4.5 \times 10^{-23})^2(45 \times 10^{-7})^3}{3(5.1 \times 10^{-21})^2}$$

$$= 11.9 \times 10^{-20} \text{ joule} \qquad \text{(D-14)}$$

We note that since $\Delta G_c \simeq \Delta_\alpha g^\dagger$

$$\Delta_\alpha g^\dagger \sim 12 \times 10^{-20} \text{ joule/molecule}$$

or

$$\Delta_\alpha g^\dagger \sim 17 \text{ kcal/mol} \qquad \text{(D-15)}$$

$\Delta_\alpha g^\dagger$ is the activation energy for addition of a mole of silicic acid to nuclei or larger particles of SiO_2. The activation energy corresponding to the energy of formation of a critical size nucleus is approximately the same.

☆U.S. GOVERNMENT PRINTING OFFICE: 1978-740-206/76